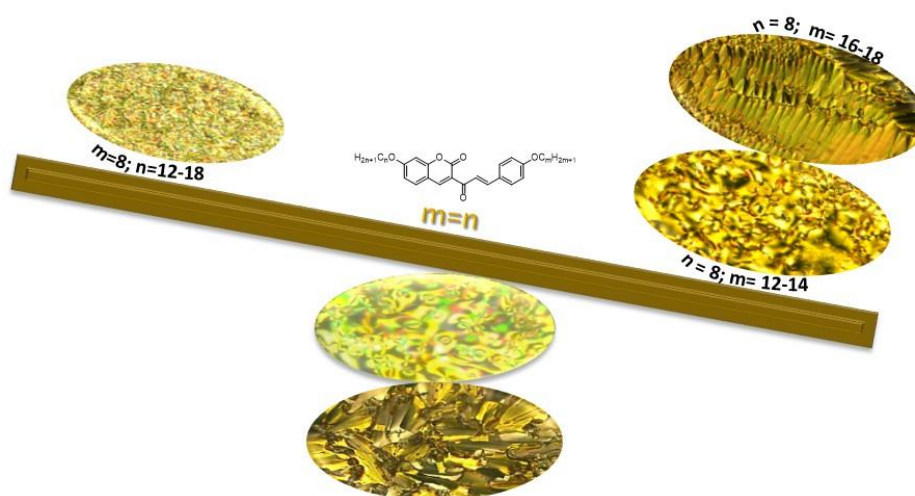


Chapter-4

Design of Unsymmetric Coumarin Chalcone Derivatives with Tunable Self-Assembling Behavior



4.1 Introduction

The Small rod like molecules play a crucial role in determining mesomorphic characteristics, and even small alterations in their configuration lead to distinct liquid crystalline phases [1-3]. The formulation of such substances involves a rigid core that incorporates multiple aromatic or heterocyclic rings. These rings are connected by diverse linking groups like azo, amido, ester, imine, chalcone, etc., and also with a flexible alkyl chain at the terminal end [4-9]. Beyond the aromatic core, the nature of the central linkage and the length of the terminal flexible chain significantly impact both thermal stability and the type and range of stability within the mesophase [10-12]. The chalcone central linkage has the potential to induce a dipole within the molecular core, similar to linkages such as ester, azo, amido, or imino. Consequently, numerous thermotropic liquid crystalline compounds featuring the chalcone linkage have been synthesized and subjected to investigation [13-19]. Chalcone linkage provides linearity in the structure as well as good thermal stability, which has significant impact on mesophase type. While variation of flexible terminal alkyl/alkoxy chain in the main core of the molecule has effect on the both physical as well as thermal properties of the molecules including melting point, phase transition temperature, mesophase type, dielectric anisotropy, dipole moment and polarizability. Recently, coumarin containing liquid crystal compounds are designed and explored as liquid crystalline materials due to several advantageous properties associated with it such as molecular stability, photo-physical properties and low energy non-covalent intermolecular interactions [20-25].

Symmetric and non-symmetric molecules along with variation of different linkages have been prepared and studied for their mesomorphic properties [26-35]. Recently, H. A. Ahmed reported non symmetrical homologues series **1a** containing Schiff base and ester linkages having two terminal alkoxy groups. All the compounds were studied for their mesophase behavior and compared with azo series **1b** (Fig-4.1) [27-28]. Compounds have shown dimorphic Smectic A and Nematic phases having more stability when substituted with higher alkoxy chain. Mohammad A. T. and Mustafa H. K. have reported two series **2a** and **2b** as unsymmetrical coumarin derivatives attached with chalcone via ether linkage (Fig-4.1) [29]. Compounds from both the series showed interesting mesomorphic properties. Thus, when there is a change in the terminal alkyl/alkoxy group, the overall rigidity of the molecules will be affected and hence the linearity will be changed as well as in intermolecular interactions. Overall, the mesogenic planar ring, central linkages and terminal alkyl chains are important in development of new compounds

In our previous work, we have also carried out synthesis of coumarin derivatives **3** and **4** with unsymmetrical terminal alkoxy chain (Fig-4.1) [30-31]. It was observed that mesophase type and stability are easily affected on varying the alkoxy group at one of terminal of the molecules. In this direction, DFT calculations can be used to evaluate crucial parameters of molecules including geometry, the frontier molecular orbitals energy, molecular electrostatic map and energy gap. The DFT calculation is one of the tool for correlation of such parameters with experimental properties of liquid crystalline compounds [32-33].

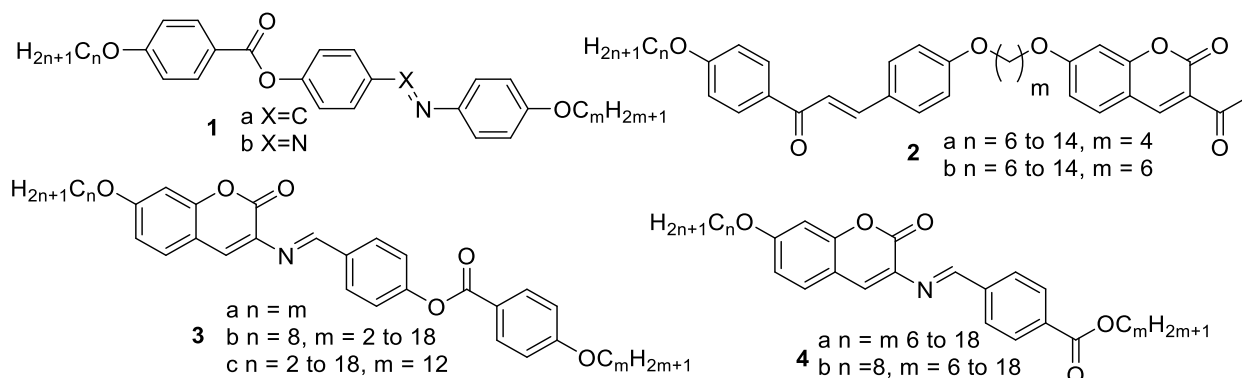


Figure- 4.1 Thermotropic mesomorphic unsymmetric derivatives

As a part of our work on the design and study of liquid crystalline compounds based on coumarin containing chalcone linkages, earlier our group has reported coumarin-chalcone derivatives with symmetric chain at both terminal of the molecule showed dimorphic properties with octyloxy chain, while lower analogues showed nematic mesophase transitions and higher analogues showed enantiotropic SmA mesophase [34]. In this particular class, all the compounds have shown fair stability of coumarin ring and chalcone central linkage in rigid core.

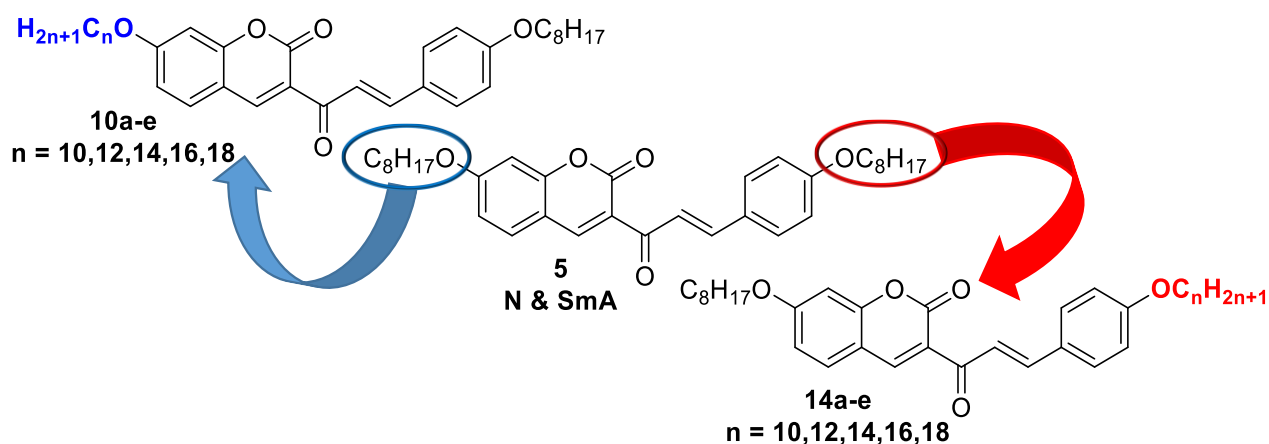


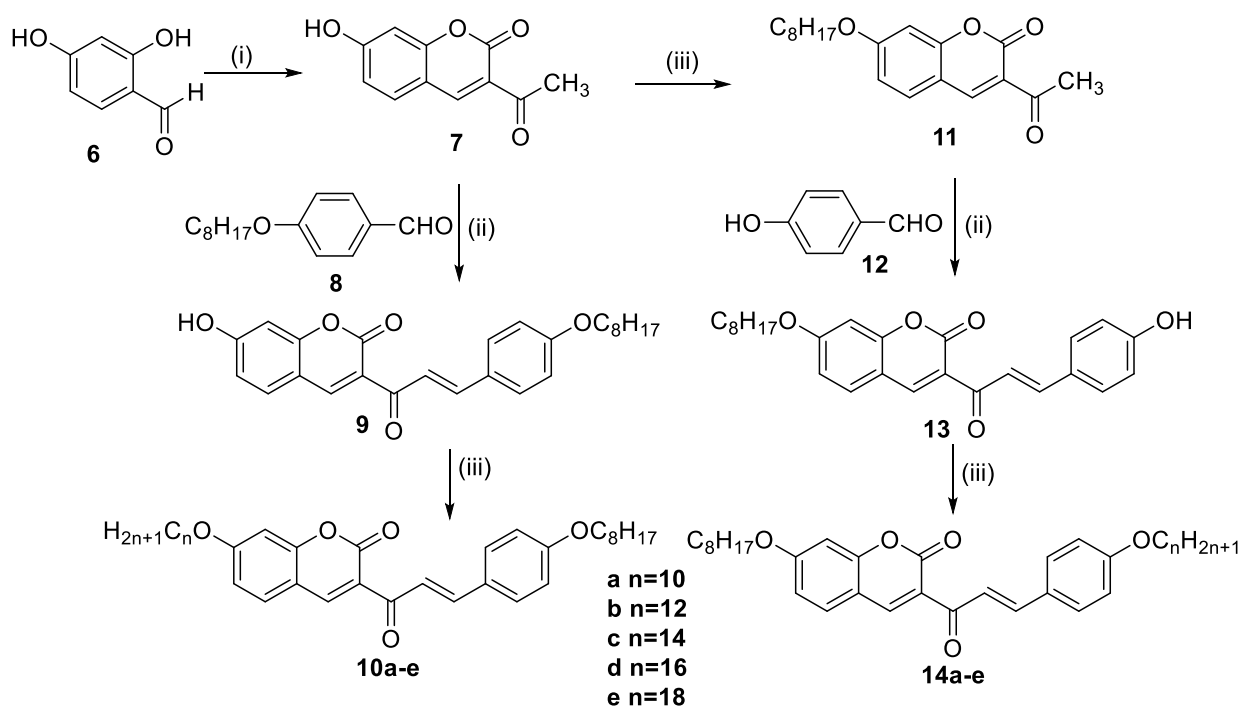
Figure- 4.2 Unsymmetric coumarin chalcone derivatives

We have selected coumain chalcone derivatives to study effect of different alkoxy chains at both ends (**Fig-4.2**). As unsymmetric terminal alkoxy groups would result in change of polarizability of chalcone linkage as well as that of the whole molecule and hence overall effect on mesomorphic properties and stability of the molecules. Further, compounds were studied for DFT calculations to obtain the various geometrical parameters, which can be used further to correlate the observed mesomorphic properties and estimated theoretical simulations.

4.2 Results and discussion

4.2.1 Chemistry

7-hydroxy-3-acetyl coumarin **7** was prepared by Knoevenagel reaction using resorcaldehyde **6** in ethanol and ethyl acetoacetate, followed by catalytic amount of piperidine and mixture was refluxed for 18 hours. Chalcone derivative **9** was prepared by condensation of compound **7** with 4-octyloxy benzaldehyde **8** (**Scheme-1**) using pyrrolidine and acetic acid by refluxing for 36 h in ethanol. Alkylation of compound **9** was carried out using different n-bromo alkanes and anhydrous K_2CO_3 using *N,N*-dimethylformamide (DMF) as solvent at 70–72 °C to form compounds **10a-e**.



Reagents and condition : (i) EAA, pyridine, piperidine, reflux, 14 h; (ii) compound **8/12**, pyrrolidine, acetic acid, ethanol, reflux, 36 h; (iii) alkyl bromide, DMF, anhy. K_2CO_3 , KI, reflux, 24 h.

Scheme 1: Synthesis of compounds **10a-e** and **14a-e**

In second variation, first compound **7** was reacted with n-octyl bromide in presence of anhydrous K_2CO_3 and pinch of KI in DMF to form 3-acetyl-7-(octyloxy)-2H-chromen-2-one

11. Further, **11** on reaction with 4-hydroxy benzaldehyde **12** and catalytic amount pyrrolidine (3-4 drops) and acetic acid in solvent ethanol by refluxing for 36 h to give chalcone derivative **13**. Compound **13** was reacted with n-alkyl bromides in presence of anhydrous K_2CO_3 in dry DMF at 70-72°C to give compounds **14a-e**. All the compounds **10a-e** and **14a-e** were characterized by using various spectral studies like IR, 1H -NMR, ^{13}C -NMR, ESI-MS and CHN analysis.

In IR spectra, all compounds **10a-e** and **14a-e** showed alkyl chain C-H stretching as two bands in the range 3096-2838 cm^{-1} . The stretching frequency of lactone coumarin was observed at 1735-1715 cm^{-1} and chalcone carbonyl stretching frequency was found to be at 1665-1648 cm^{-1} for all the compounds. 1H -NMR of compound **10b** showed methyl groups as two triplets merged at δ 0.87-0.90 ppm and methylene groups observed at δ 1.27-1.82, while $-OCH_2$ protons of both terminal alkoxy chain were observed at δ 4.01 and 4.05 as triplet. Aromatic protons of compound **10b** were observed at δ 6.84-7.93 ppm including chalcone linkage protons as two doublets at δ 7.80 and 7.91 having coupling constant value $J = 16Hz$ for trans protons. In ^{13}C -NMR of **10b** methyl group carbons at both end observed at δ 14.14 and 14.15 ppm, methylene group carbons of two alkoxy chain were observed between δ 22.68-31.90 ppm, alkoxy chain carbon next to oxygen at δ 68.17 and 69.01 ppm. Aromatic carbons of compounds **10b** were appeared from δ 100.68 to 161.46 ppm, while carbonyl carbon of lactone ring was appeared at δ 164.68 ppm and chalcone carbonyl carbon at δ 186.29 ppm. All the compounds **10a-e** and **14a-e** have shown similar pattern in 1H -NMR and ^{13}C -NMR analysis as variation were done at only chain length of terminal alkyl group at coumarin side and chalcone side of the compounds. Further all the compounds were analyzed by CHN analysis and ESI-MS analysis.

Figure- 4.3.1 IR of (E)-7-(decyloxy)-3-(3-(4-(octyloxy)phenyl)acryloyl)-2H-chromen-2-one (10a)

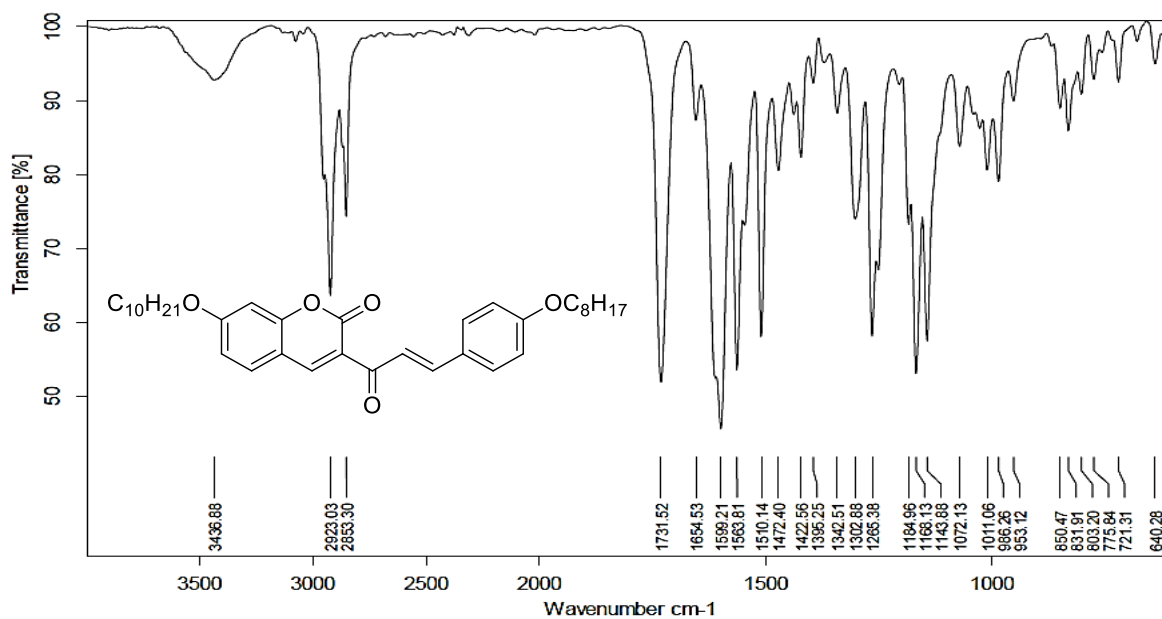


Figure- 4.3.2 1H -NMR of (E)-7-(decyloxy)-3-(3-(4-(octyloxy)phenyl)acryloyl)-2H-chromen-2-one (10a)

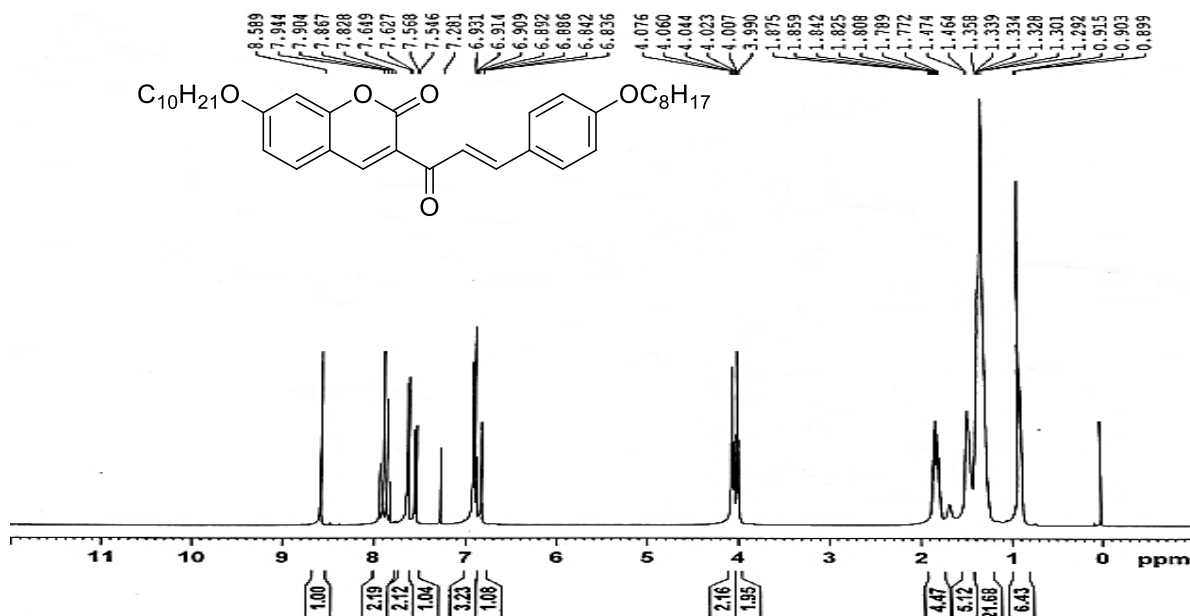


Figure- 4.3.3 ^{13}C -NMR of (E)-7-(decyloxy)-3-(3-(4-(octyloxy)phenyl)acryloyl)-2H-chromen-2-one (10a)

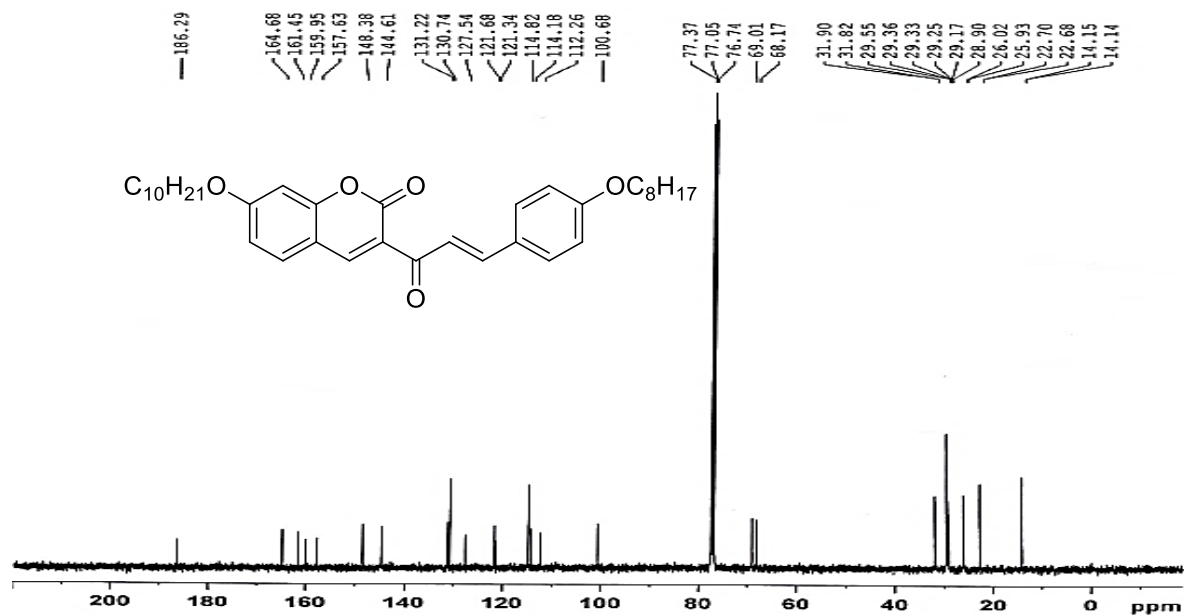


Figure- 4.4.1 IR of (E)-7-(dodecyloxy)-3-(3-(4-(octyloxy)phenyl)acryloyl)-2H-chromen-2-one (10b)

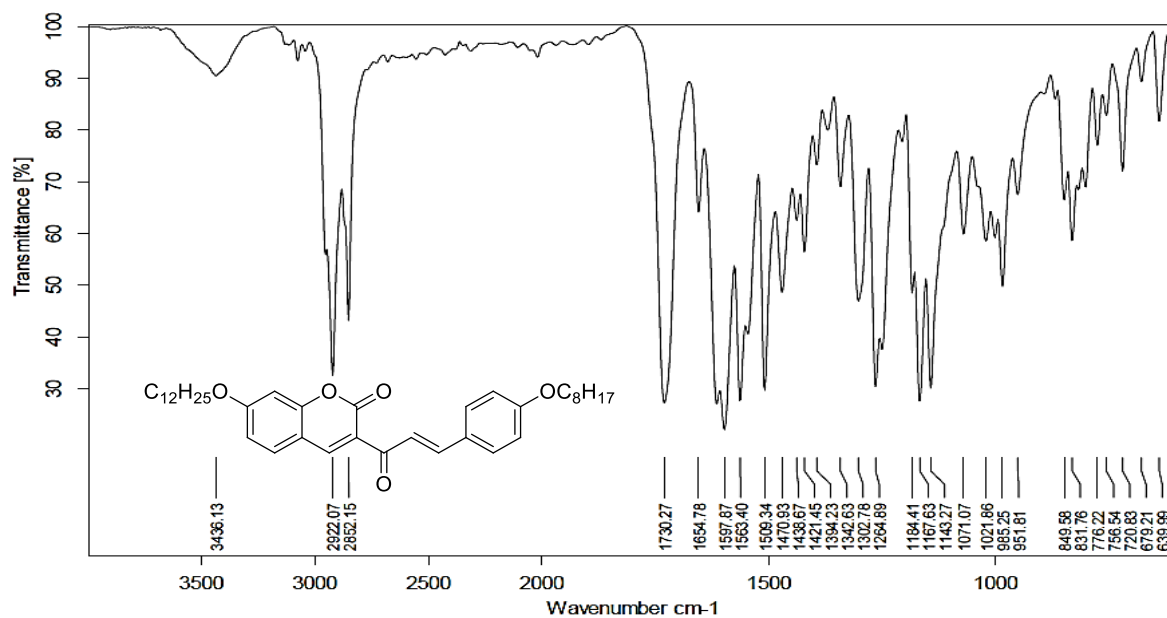


Figure- 4.4.2 $^1\text{H-NMR}$ of (E)-7-(dodecyloxy)-3-(3-(4-(octyloxy)phenyl)acryloyl)-2H-chromen-2-one (**10b**)

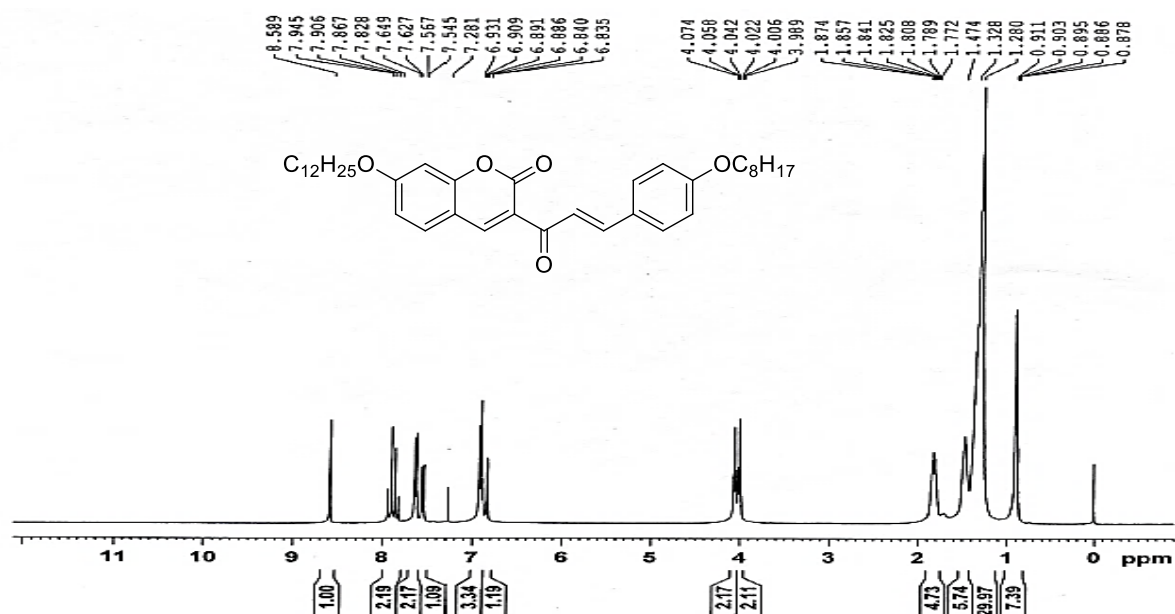


Figure- 4.4.3 $^{13}\text{C-NMR}$ of (E)-7-(dodecyloxy)-3-(3-(4-(octyloxy)phenyl)acryloyl)-2H-chromen-2-one (**10b**)

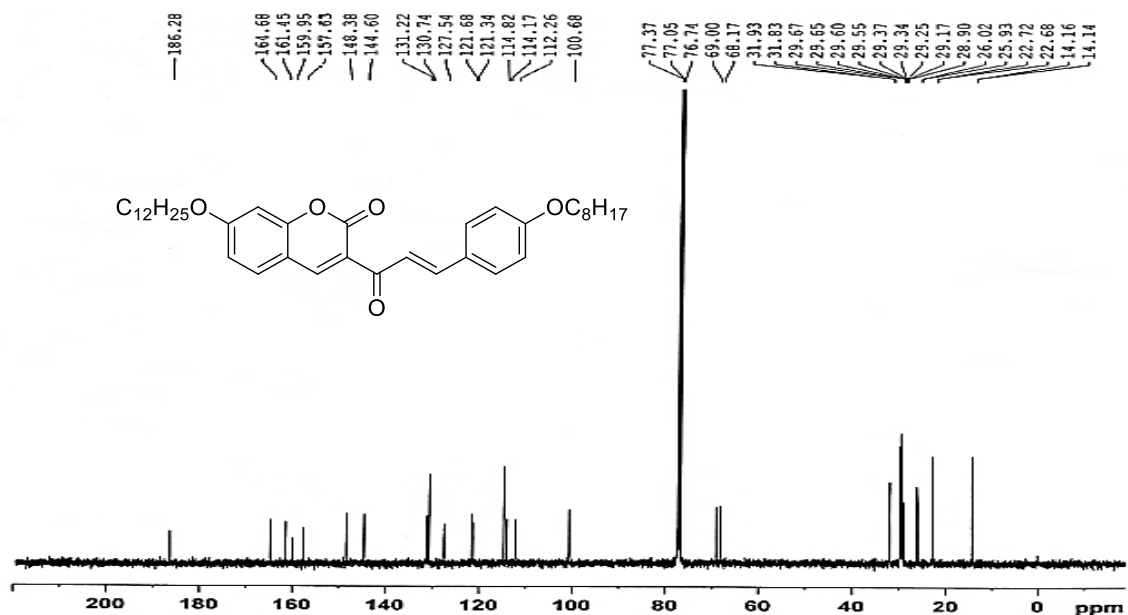


Figure- 4.5.1 IR of (E)-3-(3-(4-(octyloxy)phenyl)acryloyl)-7-(tetradecyloxy)-2H-chromen-2-one (10c)

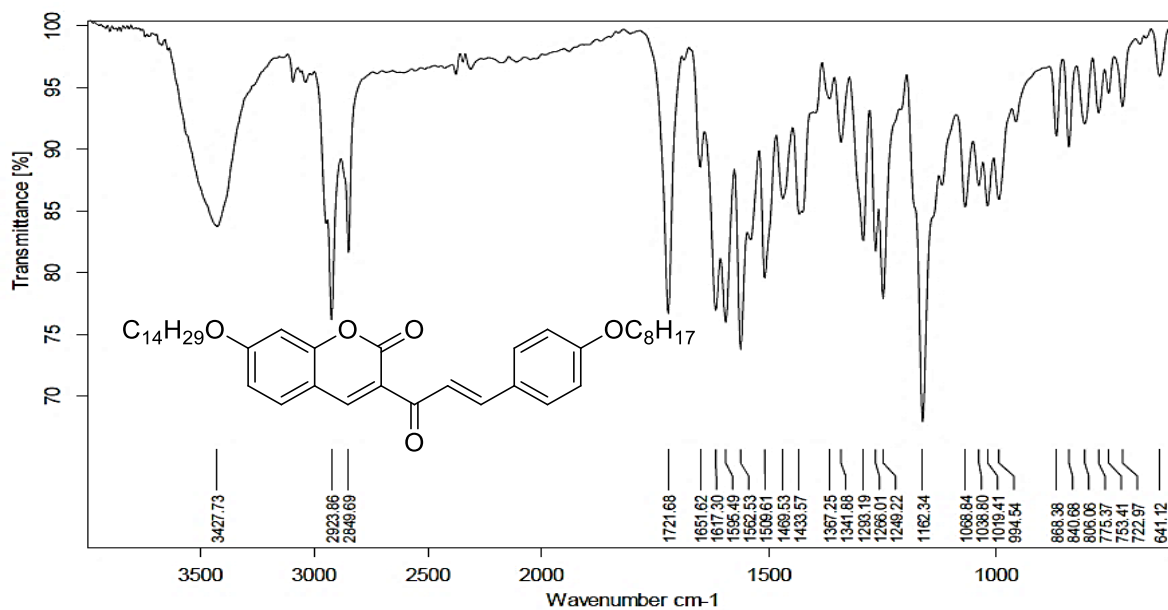


Figure- 4.5.2 $^1\text{H-NMR}$ of (E)-3-(3-(4-(octyloxy)phenyl)acryloyl)-7-(tetradecyloxy)-2H-chromen-2-one (10c)

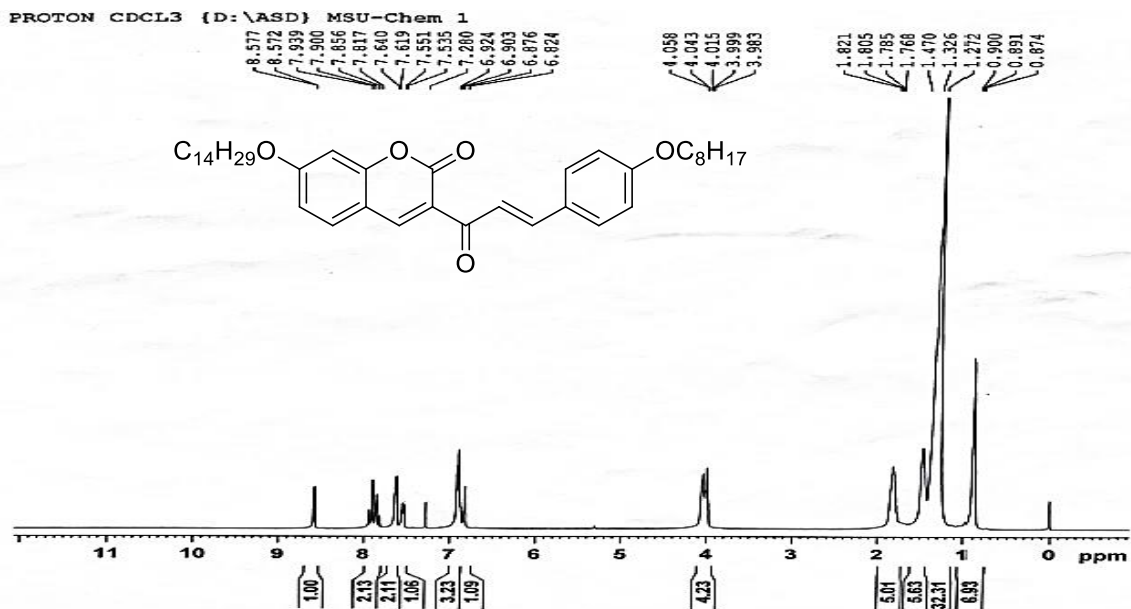


Figure- 4.5.3 ^{13}C -NMR of (E)-3-(3-(4-(octyloxy)phenyl)acryloyl)-7-(tetradecyloxy)-2H-chromen-2-one (**10c**)

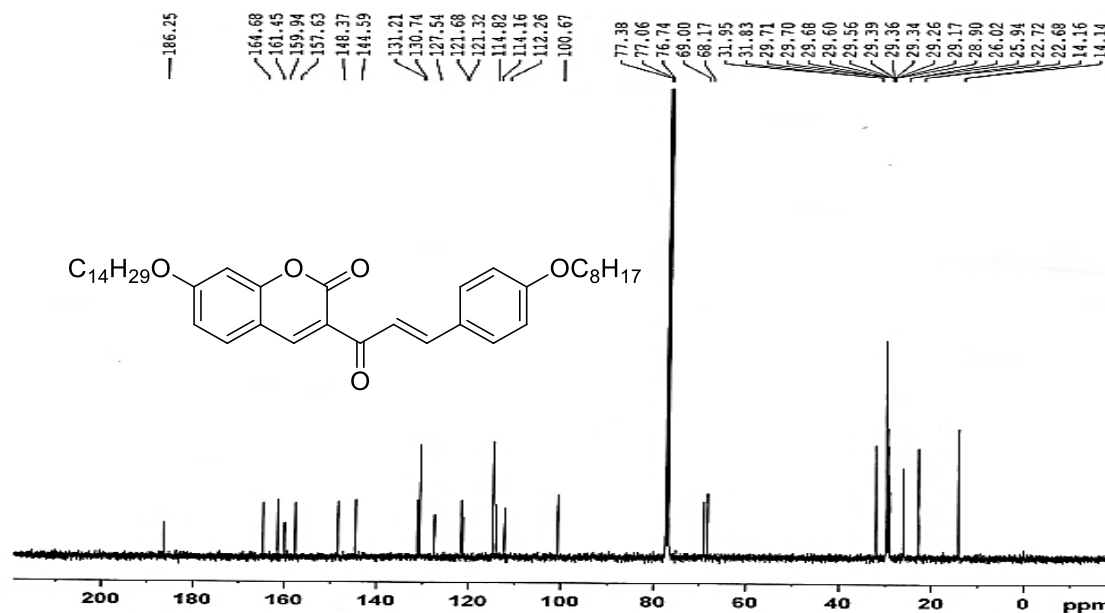


Figure- 4.6.1 IR of (E)-7-(hexadecyloxy)-3-(3-(4-(octyloxy)phenyl)acryloyl)-2H-chromen-2-one (**10d**)

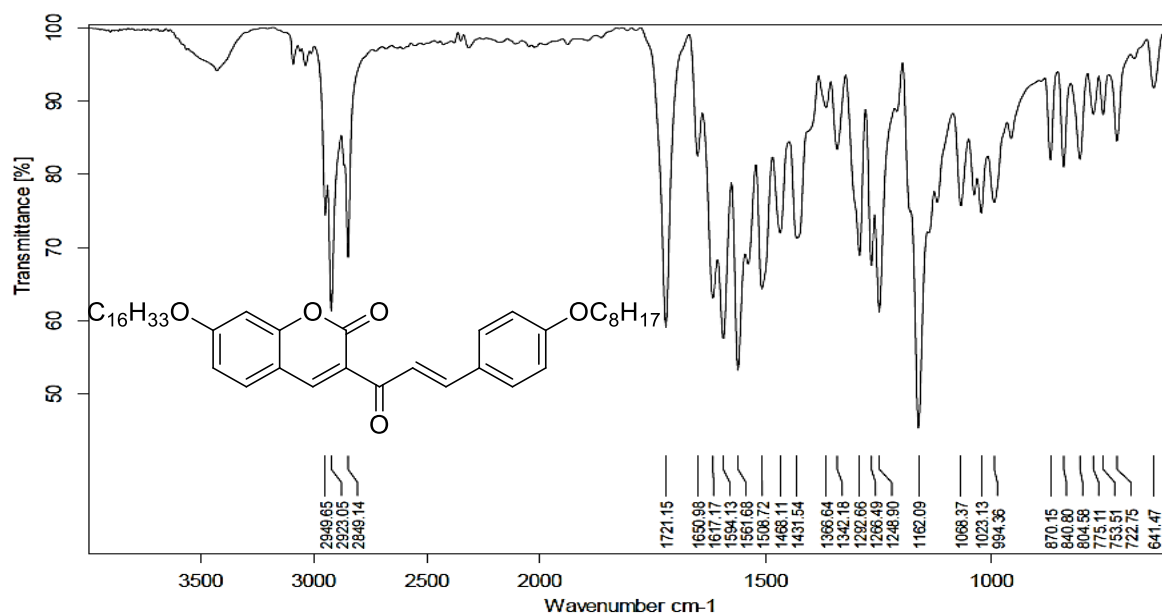


Figure- 4.6.2 $^1\text{H-NMR}$ of (E)-7-(hexadecyloxy)-3-(3-(4-(octyloxy)phenyl)acryloyl)-2H-chromen-2-one (**10d**)

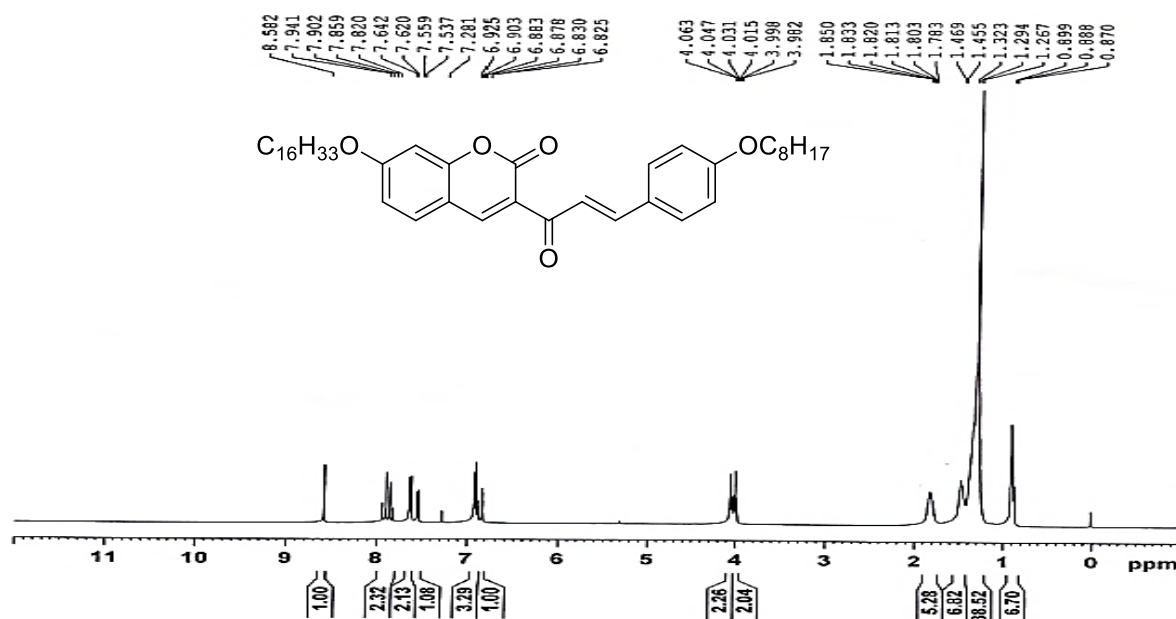


Figure- 4.6.3 $^{13}\text{C-NMR}$ of (E)-7-(hexadecyloxy)-3-(3-(4-(octyloxy)phenyl)acryloyl)-2H-chromen-2-one (**10d**)

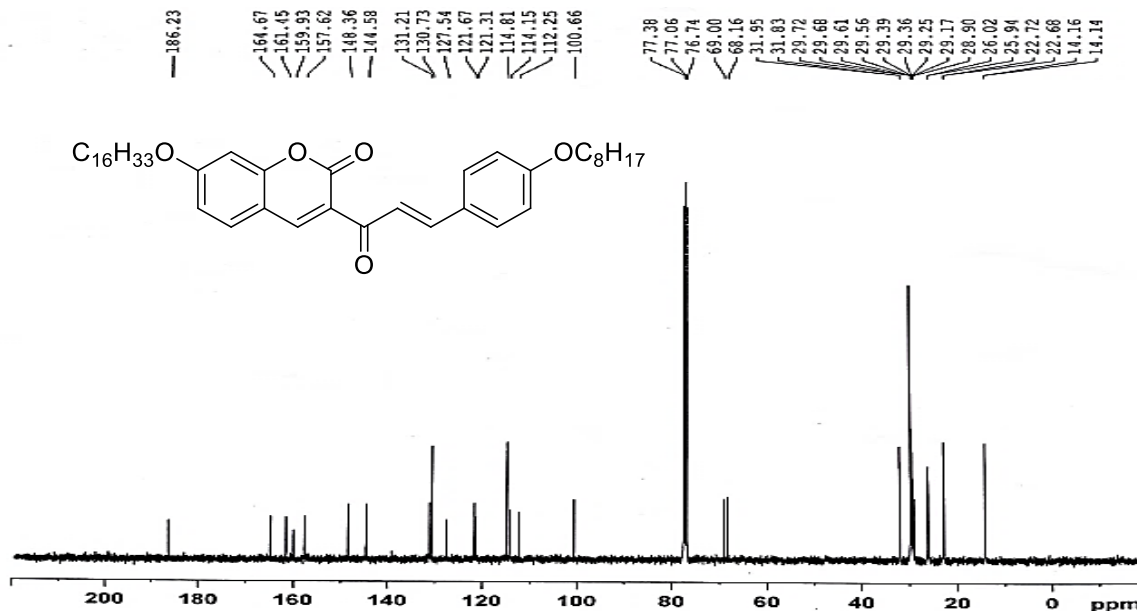


Figure- 4.7.1 IR of (E)-7-(octadecyloxy)-3-(3-(4-(octyloxy)phenyl)acryloyl)-2H-chromen-2-one (10e)

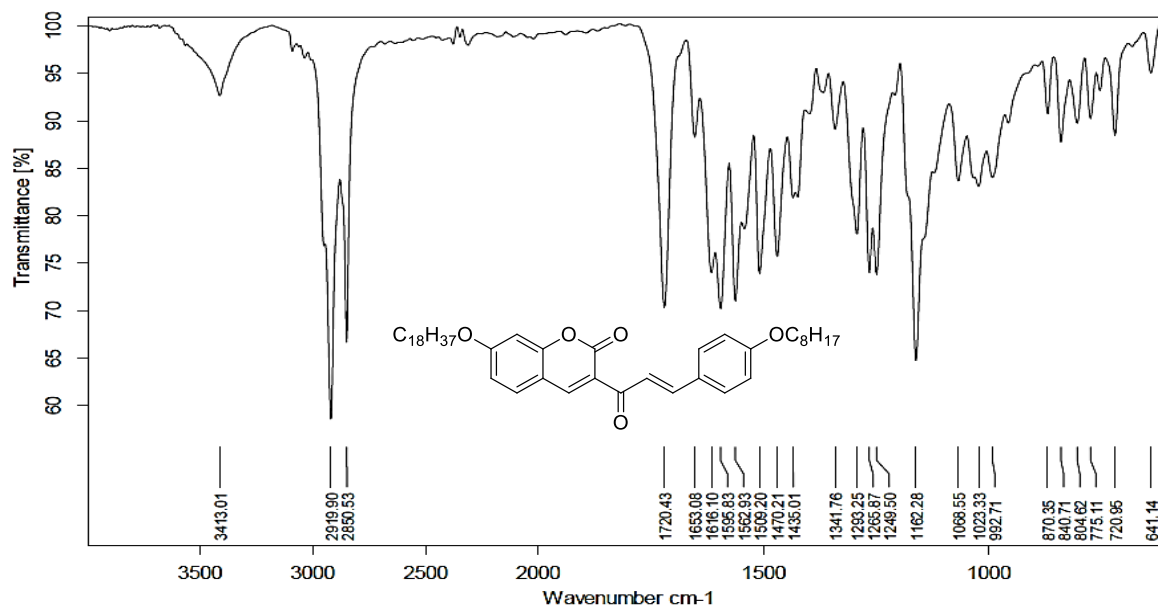


Figure- 4.7.2 ¹H-NMR of (E)-7-(octadecyloxy)-3-(3-(4-(octyloxy)phenyl)acryloyl)-2H-chromen-2-one (10e)

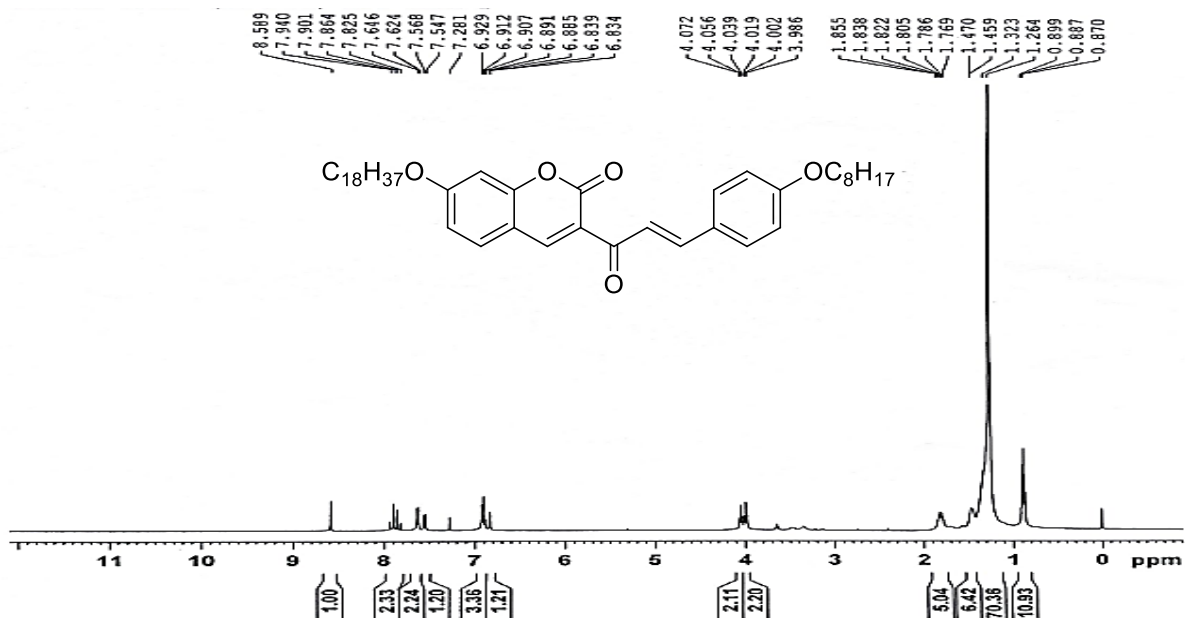


Figure- 4.7.3 ^{13}C -NMR of (E)-7-(octadecyloxy)-3-(3-(4-(octyloxy)phenyl)acryloyl)-2H-chromen-2-one (**10e**)

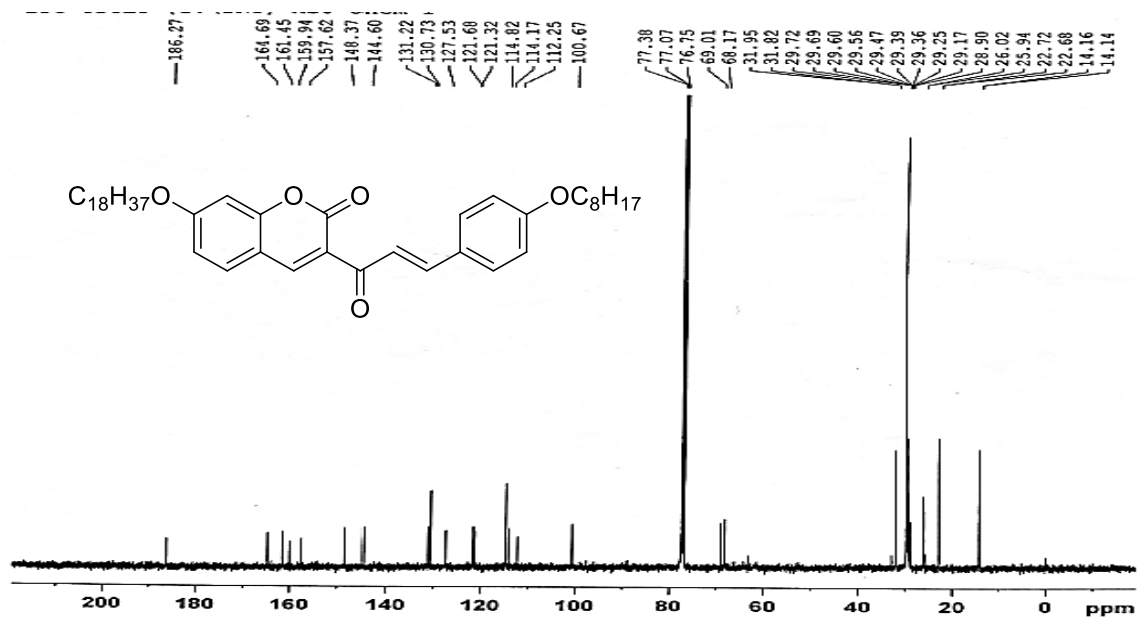


Figure- 4.8.1 IR of (E)-3-(3-(4-hydroxyphenyl)acryloyl)-7-(octyloxy)-2H-chromen-2-one (**13**)

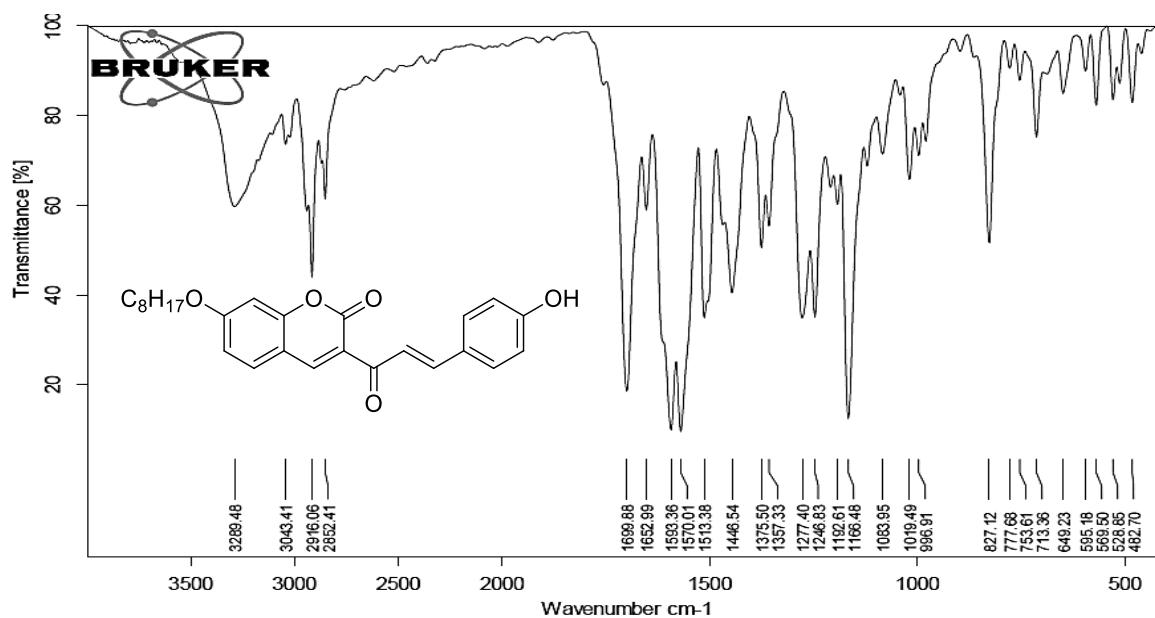


Figure- 4.8.2 $^1\text{H-NMR}$ of (E)-3-(3-(4-hydroxyphenyl)acryloyl)-7-(octyloxy)-2H-chromen-2-one (13)

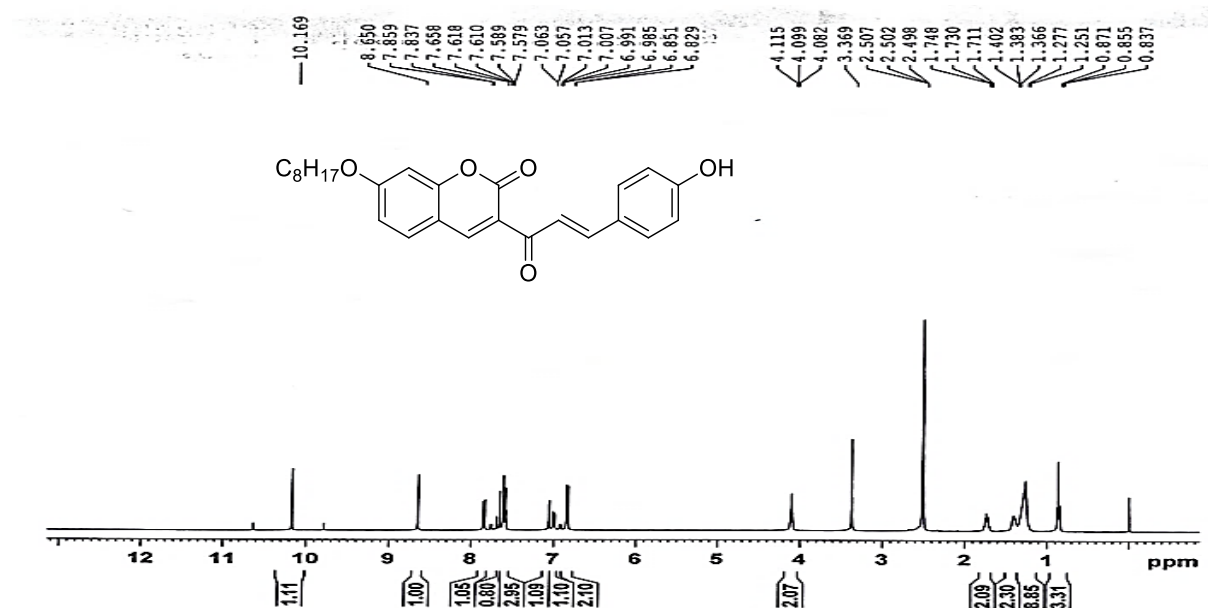


Figure- 4.8.3 $^{13}\text{C-NMR}$ of (E)-3-(3-(4-hydroxyphenyl)acryloyl)-7-(octyloxy)-2H-chromen-2-one (13)

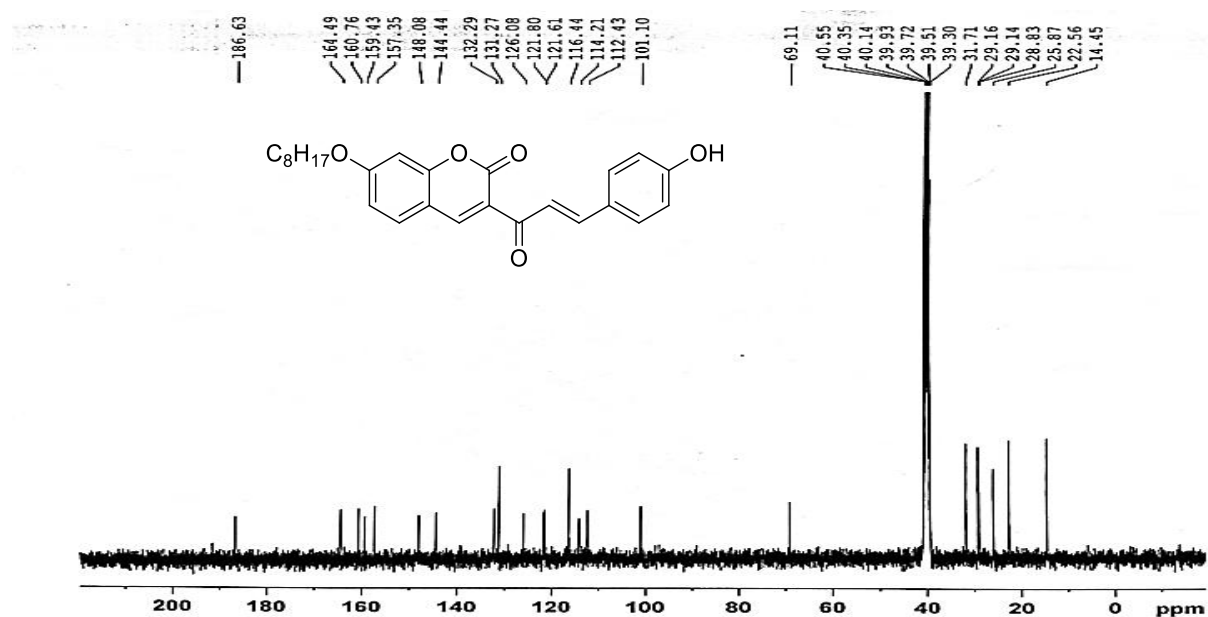


Figure- 4.8.4 Mass of (E)-3-(3-(4-hydroxyphenyl)acryloyl)-7-(octyloxy)-2H-chromen-2-one (13) M+H peak at 421.2

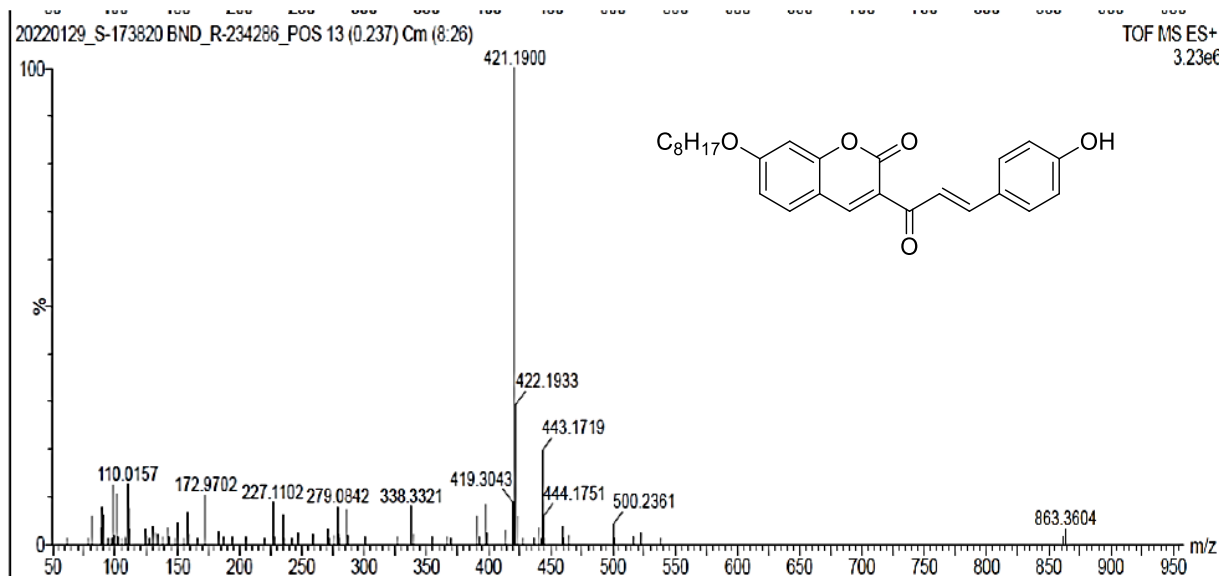


Figure- 4.9.1 IR of (E)-3-(3-(4-(decyloxy)phenyl)acryloyl)-7-(octyloxy)-2H-chromen-2-one (14a)

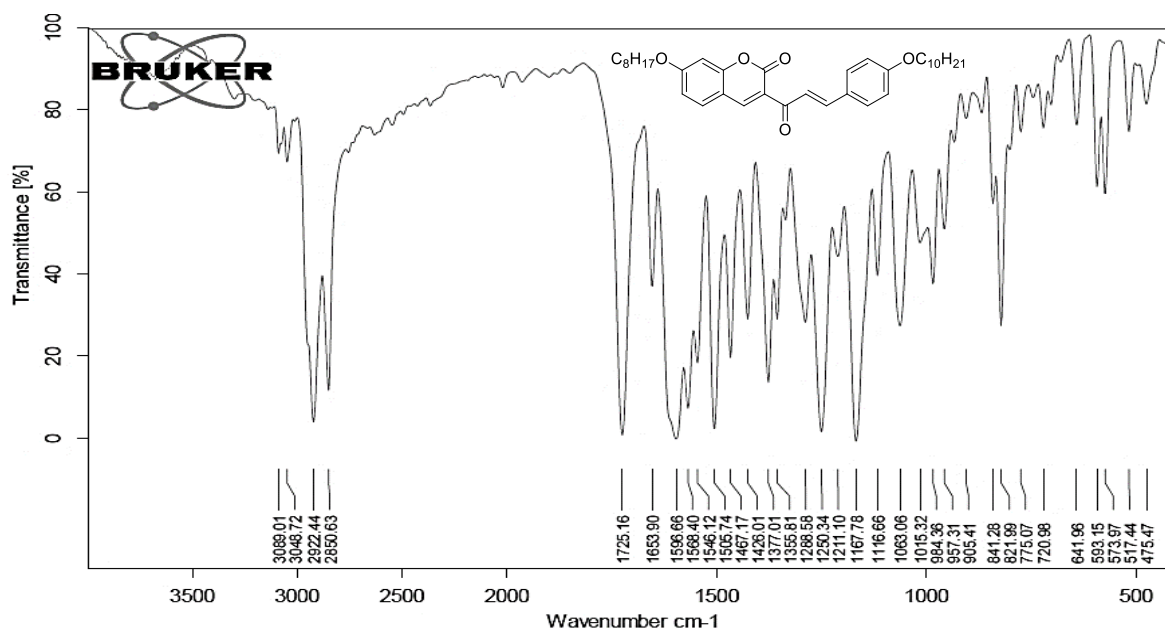


Figure- 4.9.2 $^1\text{H-NMR}$ of (E)-3-(3-(4-(decyloxy)phenyl)acryloyl)-7-(octyloxy)-2H-chromen-2-one (14a)

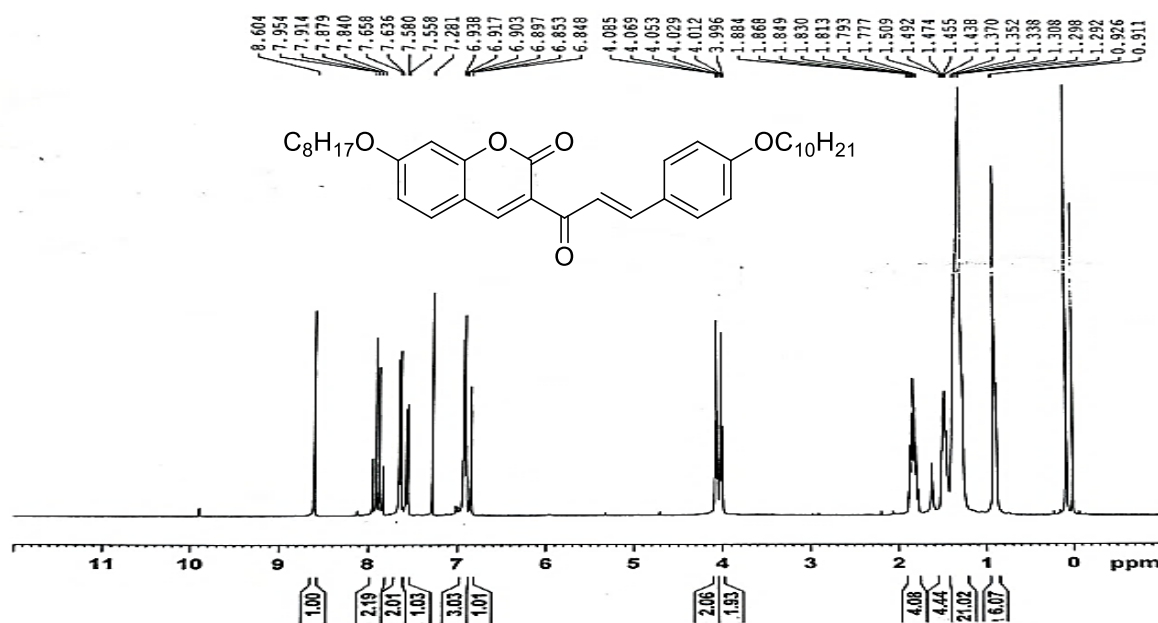


Figure- 4.9.3 $^{13}\text{C-NMR}$ of (E)-3-(3-(4-(decyloxy)phenyl)acryloyl)-7-(octyloxy)-2H-chromen-2-one (14a)

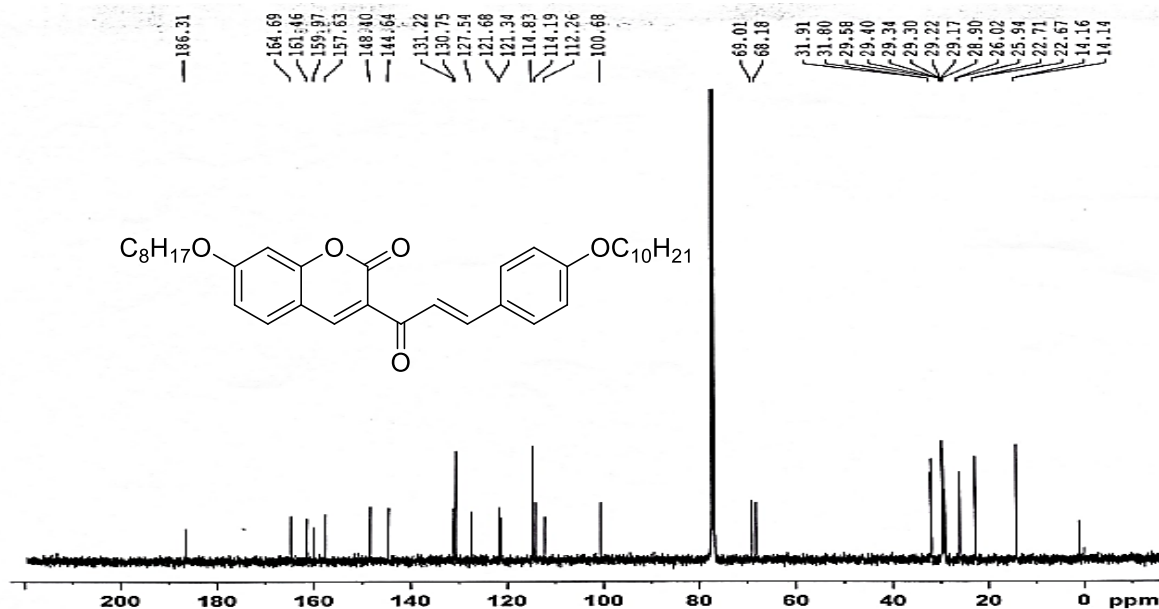


Figure- 4.9.4 Mass of (E)-3-(3-(4-(decyloxy)phenyl)acryloyl)-7-(octyloxy)-2H-chromen-2-one (**14a**) M+H peak at 561.36

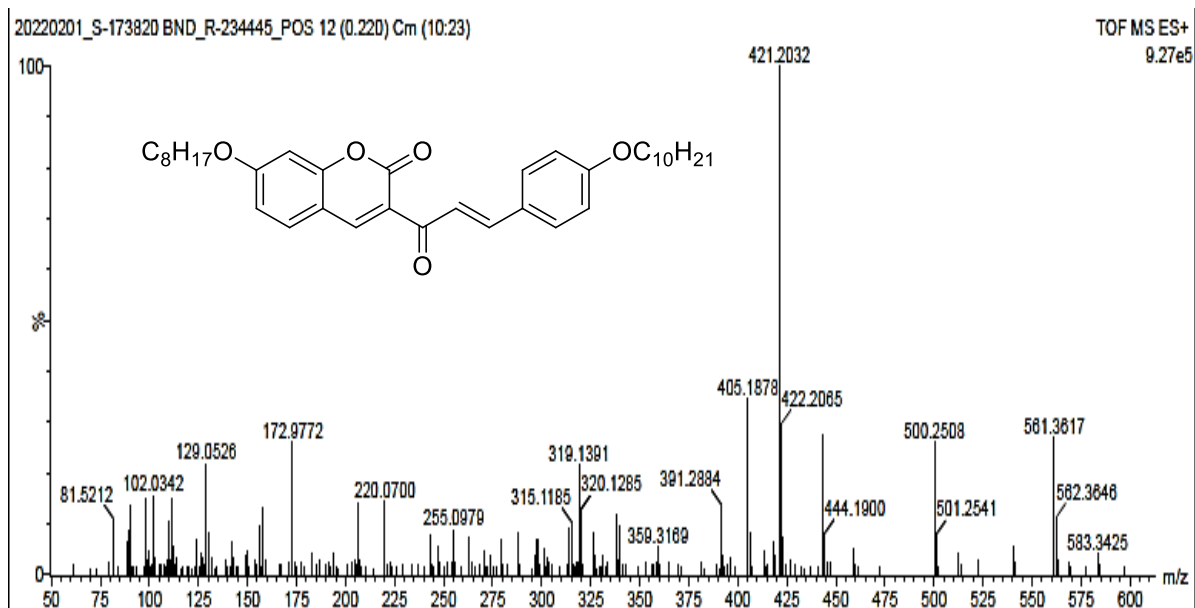


Figure- 4.10.1 IR of (E)-3-(3-(4-(dodecyloxy)phenyl)acryloyl)-7-(octyloxy)-2H-chromen-2-one (**14b**)

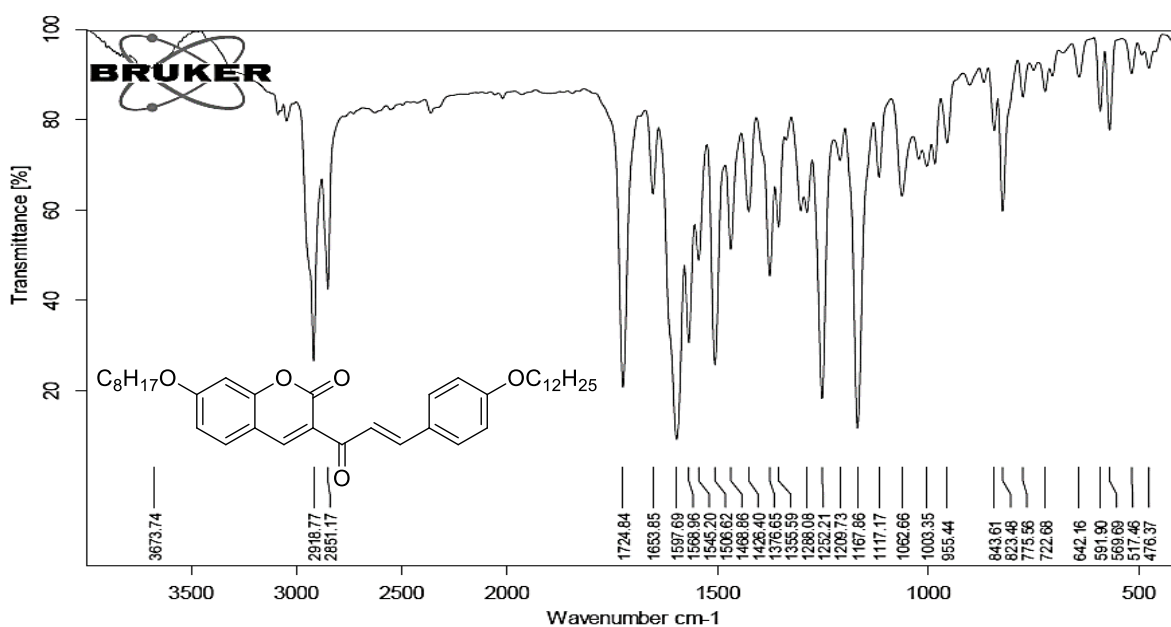


Figure- 4.10.2 $^1\text{H-NMR}$ of (E)-3-(3-(4-(dodecyloxy)phenyl)acryloyl)-7-(octyloxy)-2H-chromen-2-one (**14b**)

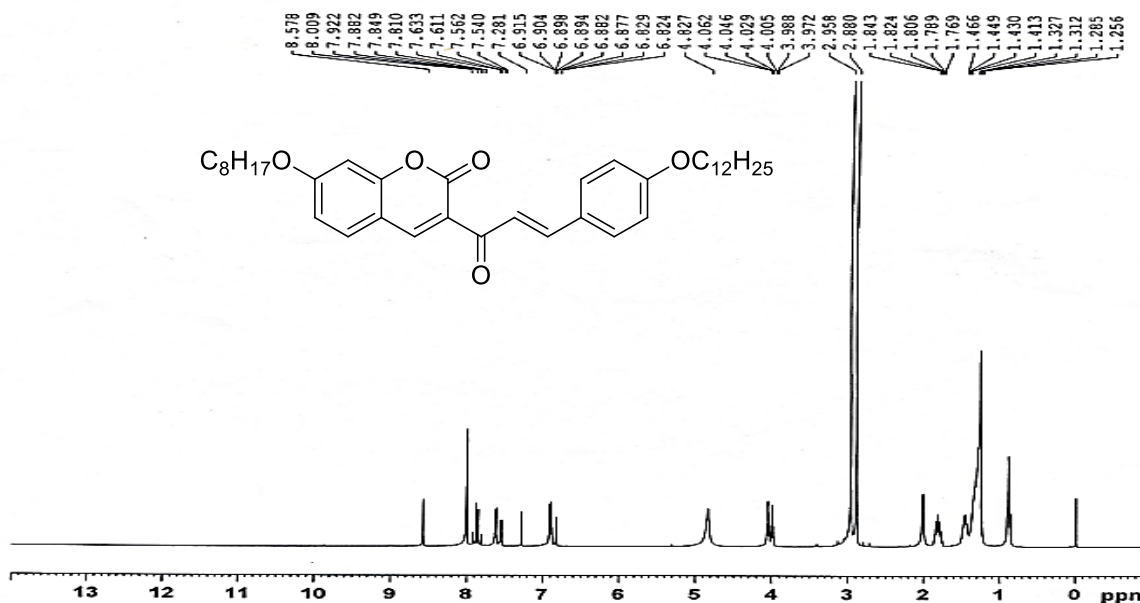


Figure- 4.10.3 $^{13}\text{C-NMR}$ of (E)-3-(3-(4-(dodecyloxy)phenyl)acryloyl)-7-(octyloxy)-2H-chromen-2-one (**14b**)

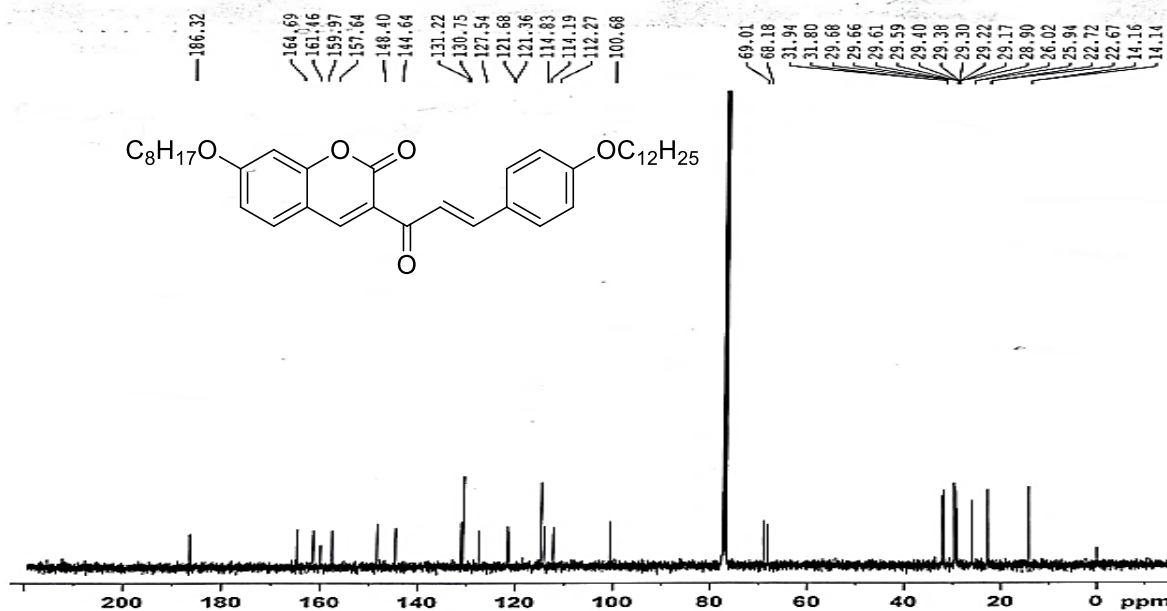


Figure- 4.10.4 Mass of (E)-3-(3-(4-(dodecyloxy)phenyl)acryloyl)-7-(octyloxy)-2H-chromen-2-one (**14b**) M-H peak at 587.30

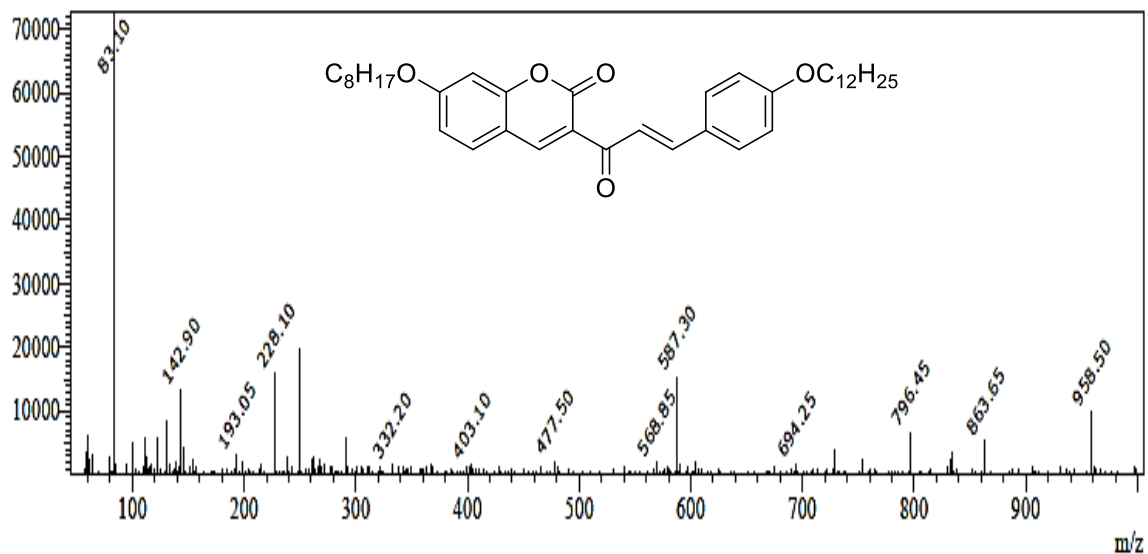


Figure- 4.11.1 IR of (E)-3-(3-(4-(octyloxy)phenyl)acryloyl)-7-(tetradecyloxy)-2H-chromen-2-one (**14c**)

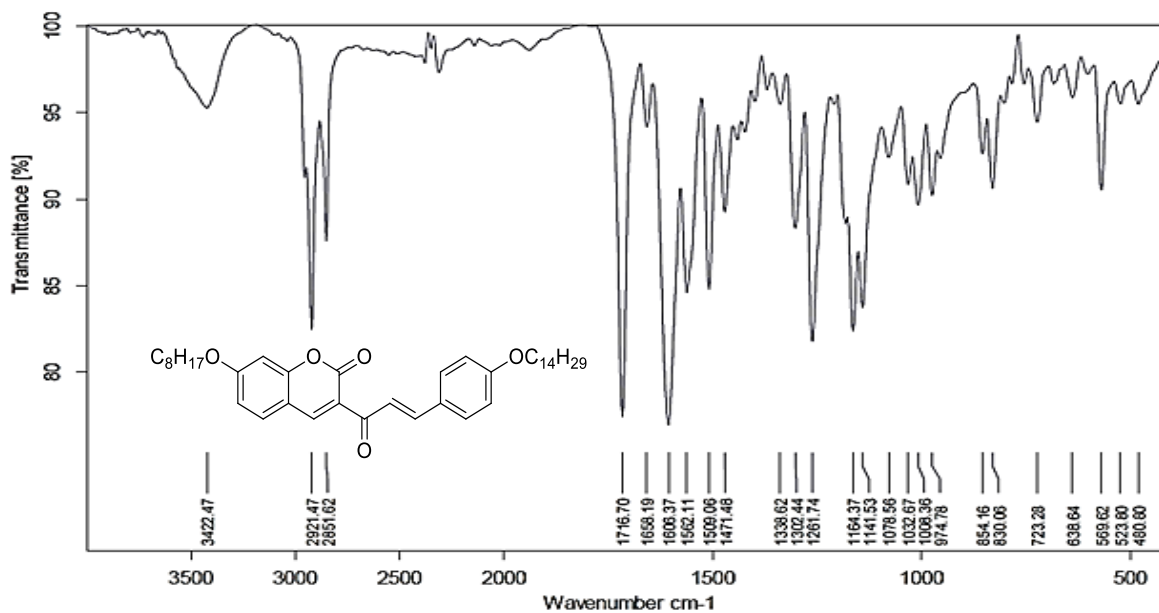


Figure- 4.11.2 $^1\text{H-NMR}$ of (E)-3-(3-(4-(octyloxy)phenyl)acryloyl)-7-(tetradecyloxy)-2H-chromen-2-one (**14c**)

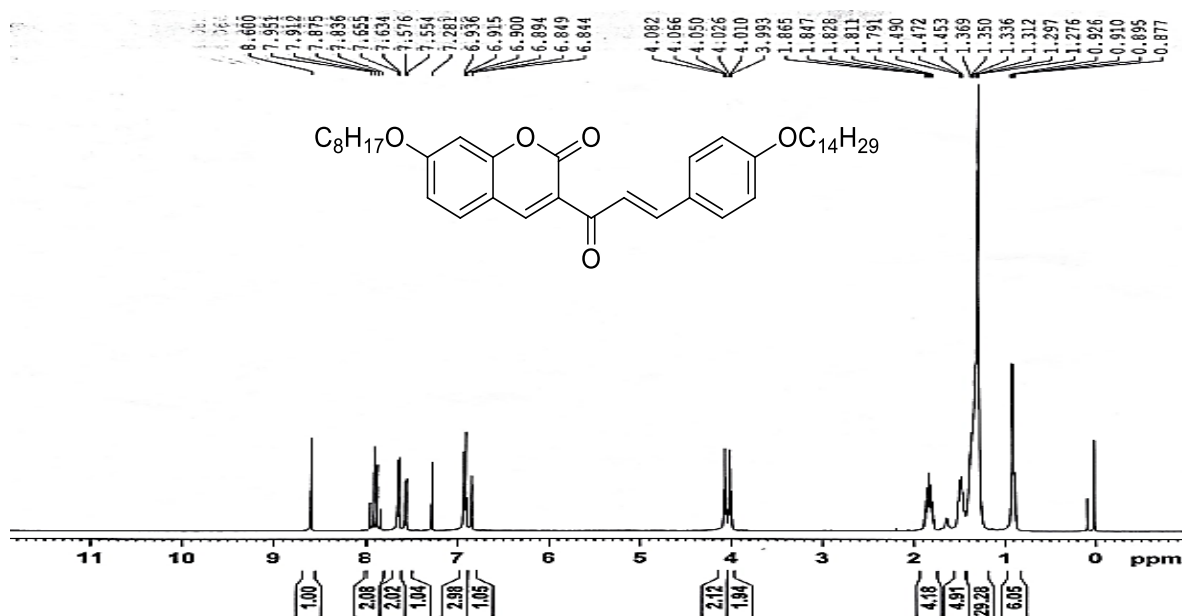


Figure- 4.12.1 IR of (E)-3-(3-(4-(hexadecyloxy)phenyl)acryloyl)-7-(octyloxy)-2H-chromen-2-one (14d)

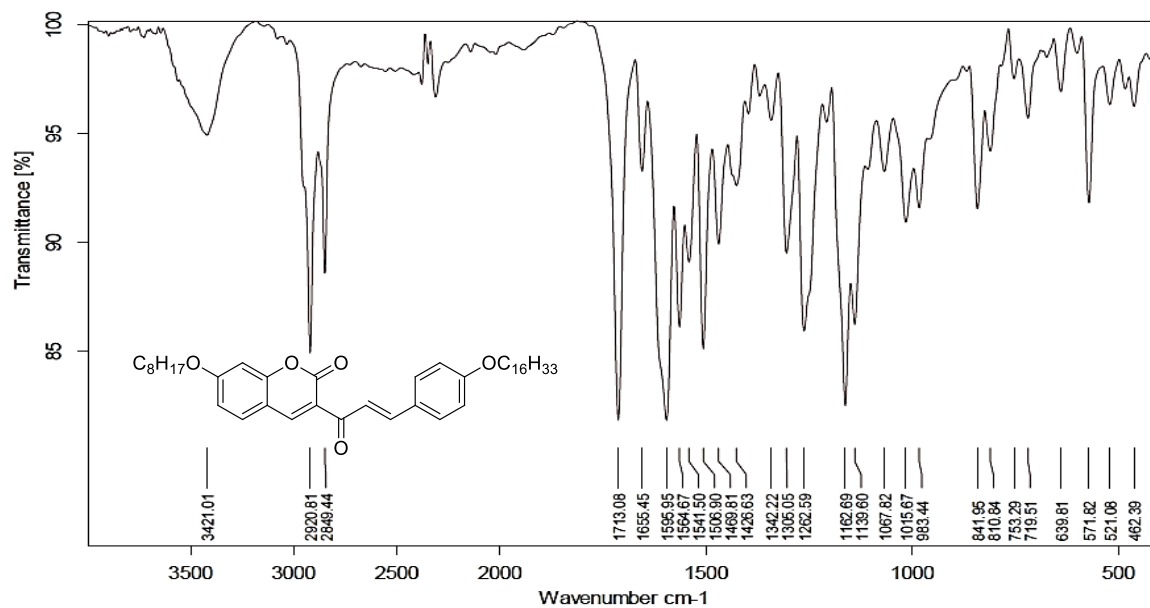


Figure- 4.12.2 $^1\text{H-NMR}$ of (E)-3-(3-(4-(hexadecyloxy)phenyl)acryloyl)-7-(octyloxy)-2H-chromen-2-one (14d)

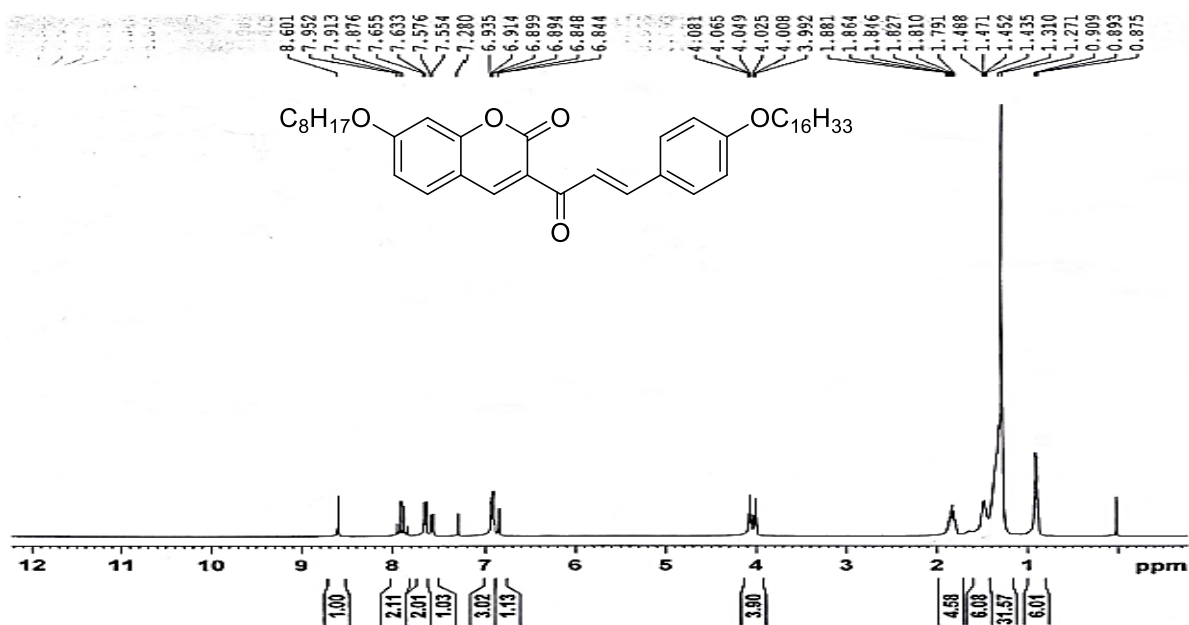


Figure- 4.12.3 ^{13}C -NMR of (E)-3-(3-(4-(hexadecyloxy)phenyl)acryloyl)-7-(octyloxy)-2H-chromen-2-one (**14d**)

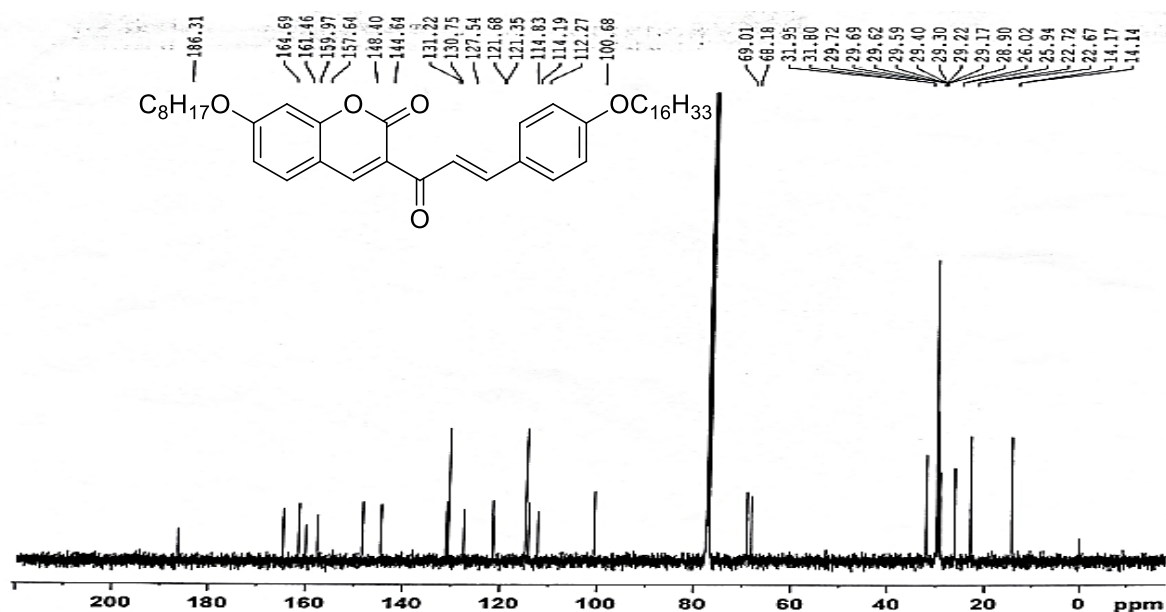


Figure- 4.13.1 IR of (E)-3-(3-(4-(octadecyloxy)phenyl)acryloyl)-7-(octyloxy)-2H-chromen-2-one (**14e**)

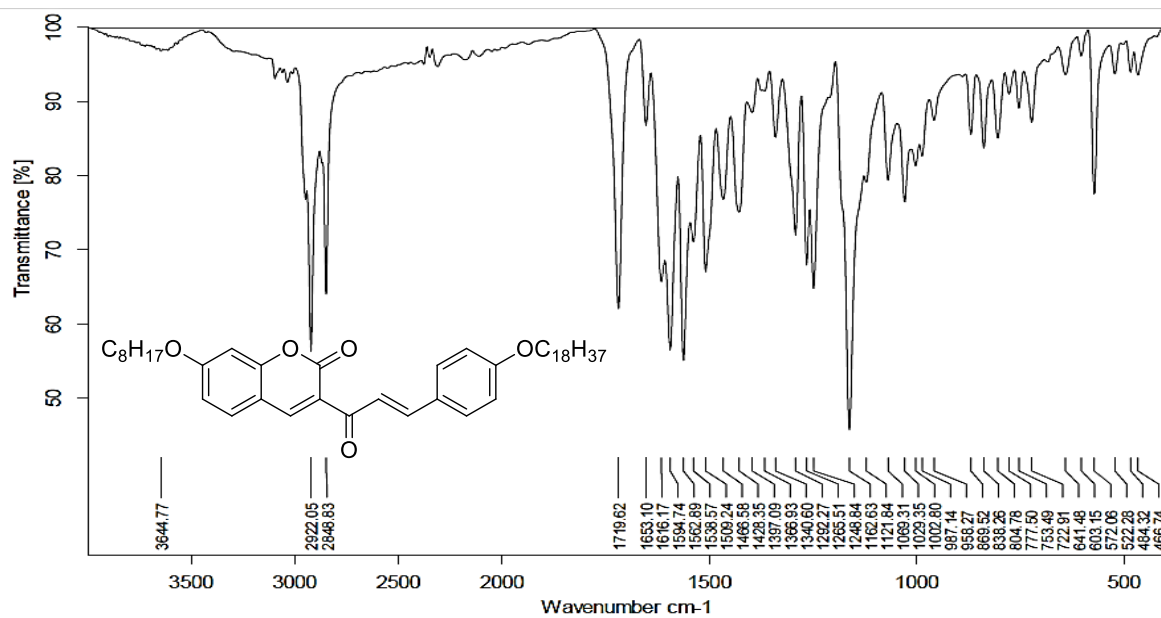


Figure- 4.13.2 $^1\text{H-NMR}$ of (E)-3-(3-(4-(octadecyloxy)phenyl)acryloyl)-7-(octyloxy)-2H-chromen-2-one (**14e**)

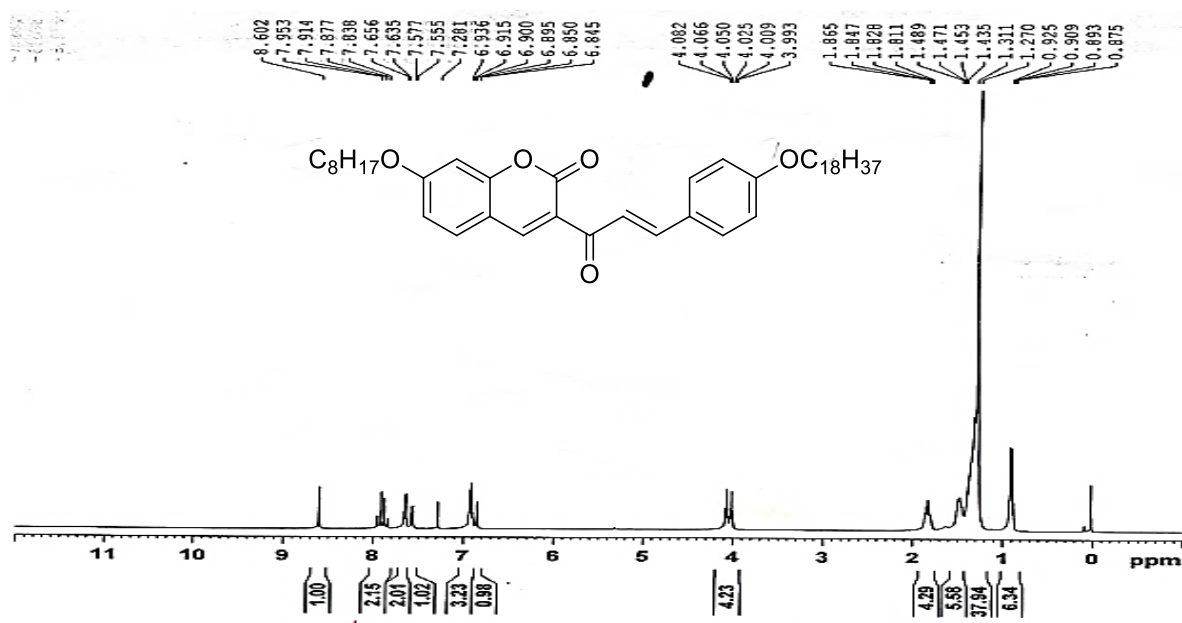


Figure- 4.13.3 $^{13}\text{C-NMR}$ of (E)-3-(3-(4-(octadecyloxy)phenyl)acryloyl)-7-(octyloxy)-2H-chromen-2-one (**14e**)

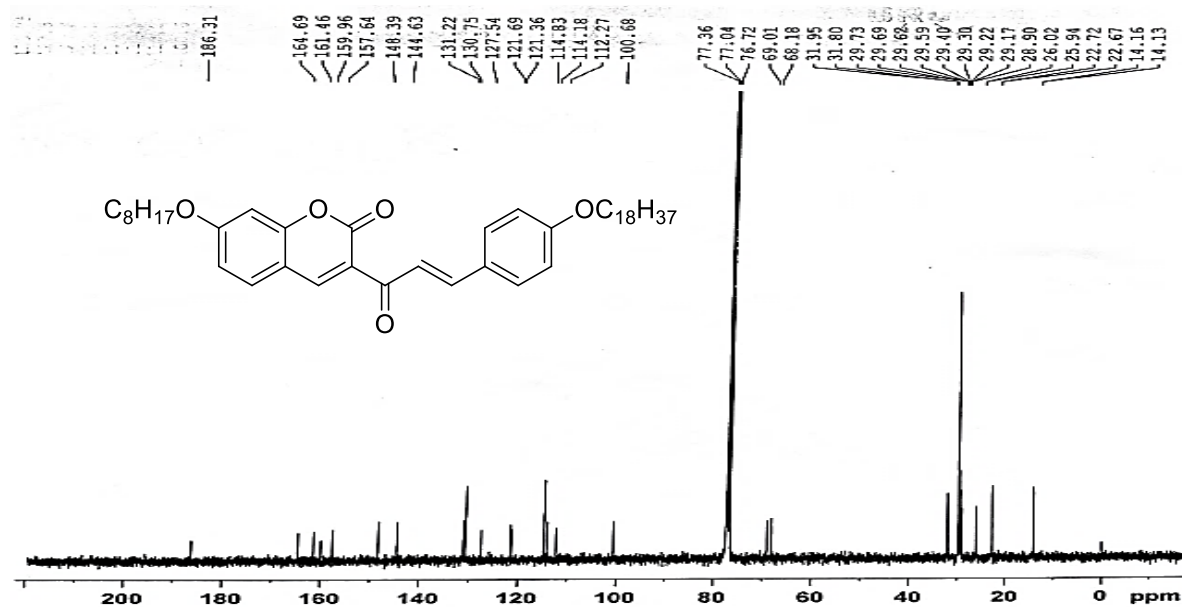
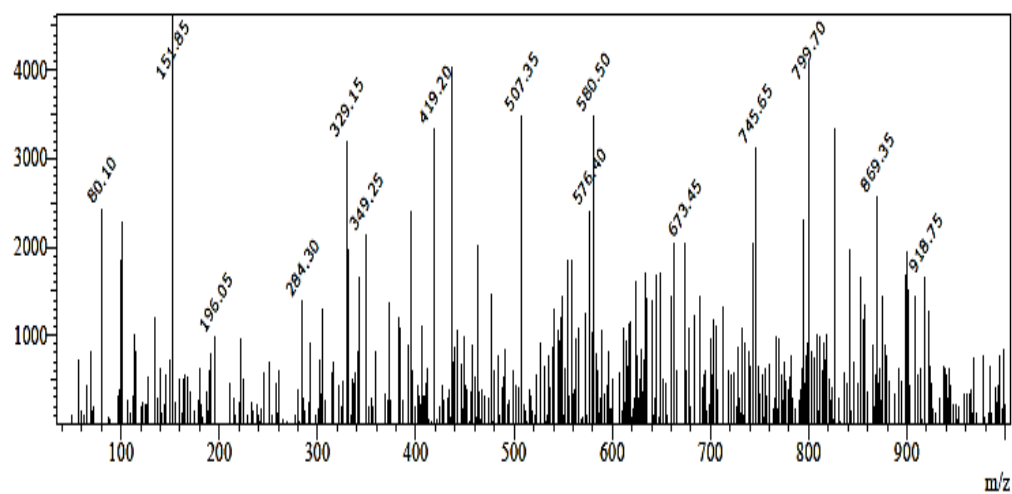


Figure- 4.13.4 Mass of (E)-3-(3-(4-(octadecyloxy)phenyl)acryloyl)-7-(octyloxy)-2H-chromen-2-one (**14e**) M+H peak at 673.45



4.2.2 Study of mesomorphic properties:

Compounds **10a-e** and **14a-e** were analysed using polarizing optical microscope for mesophase identification and optical textures. For POM analysis, thin film of compound was studied at the rate of 10 °C/min during 1st cooling and 2nd heating cycle and textures formed were identified. Further, all the compounds were analysed using differential scanning calorimetry (DSC) to calculate thermograms in heating and cooling scan at the rate of 10 °C/min. DSC curves have shown clear transition temperatures, while good mesophase textures were obtained from POM analysis for all the studied compounds for multiple heating and cooling cycles (**Table 4.1**).

4.2.2.1 Polarizing optical microscopy (POM) study:

Chalcone derivatives of coumarin with successive increase of alkyl group at two sides of the molecules were studied earlier from our group and compounds with octyloxy group showed stable SmA and nematic mesophase during heating and cooling cycle respectively. Hence, octyloxy chain length was selected to explore the effect of change in alkyl group of two sides of the coumarin chalcone molecules. In the first homologous series, compounds **10a-e** have been analyzed for their mesomorphic properties with octyloxy chain on chalcone end and varied alkoxy chain length $n = 10, 12, 14, 16, 18$ at coumarin end of the molecule. In this series, compound **10a** with decyloxy chain exhibited nematic mesophase only in cooling cycle (**Fig- 4.3a-b**), while enantiotropic SmC mesophase on both heating and cooling. On changing the decyloxy with higher alkoxy chain length, compounds **10b-e** showed enantiotropic SmC mesophase.

In second homologous series, compounds **14a-e** have been analyzed for their mesomorphic properties and varied alkoxy chain length $n = 10, 12, 14, 16, 18$ at chalcone end of the molecule. In this series, monotropic nematic mesophase was observed from compounds **14a-b** with decyloxy and dodecyloxy chain length respectively (**Fig- 4.3d**). Compound **14c** with tetradecyloxy exhibited enantiotropic nematic mesophase (**Fig- 4.3d**), While both the compounds **14d** and **14e** showed enantiotropic SmA mesophase (**Fig- 4.3f**).

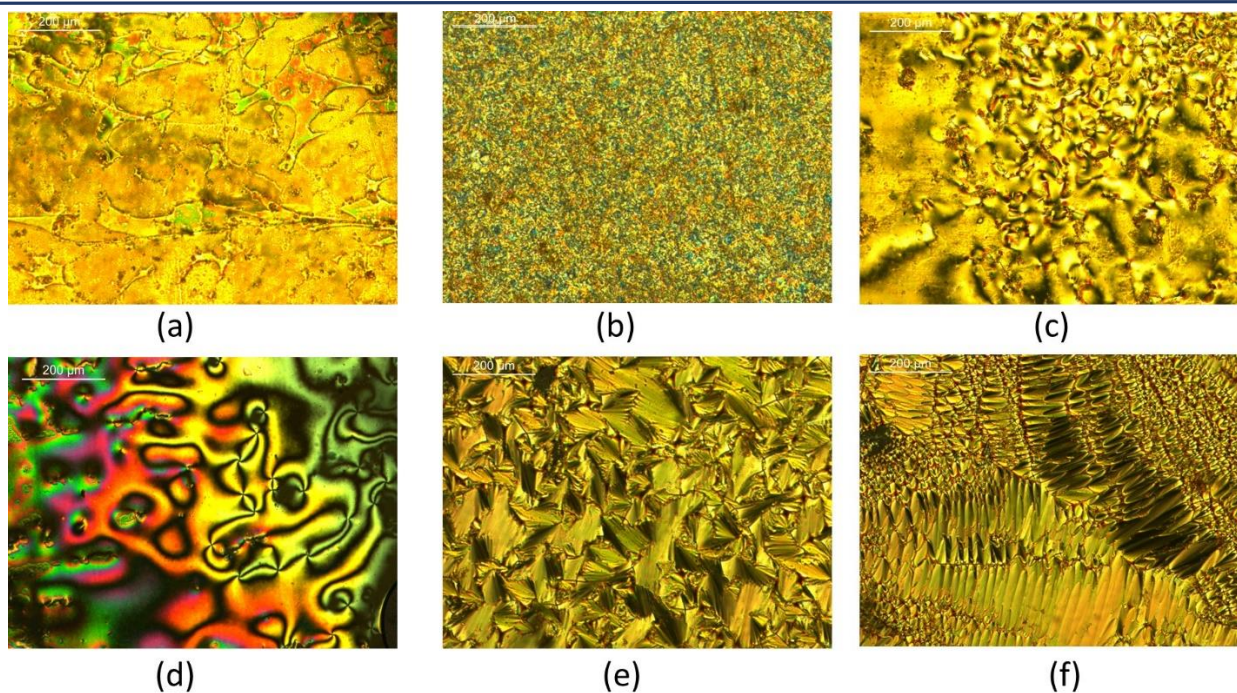
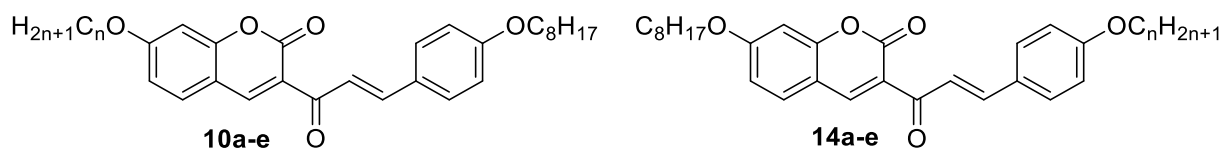


Figure- 4.3 Liquid crystal phase transition (a) nematic marble for compound **10a** on cooling (b) SmC broken fan texture **10d** (c) nematic marble for compound **14a** (d) nematic schlieren texture for compound **14c** (e) SmA focal conic for compound **14d** in cooling cycle (f) SmA focal conic for compound **14d** in heating cycle

4.2.2.2 Differential scanning calorimetry study (DSC):

Unsymmetric coumarin chalcone derivatives **10a-e** and **14a-e** have been analyzed for transition temperatures and associated enthalpy values using DSC during both heating scan and cooling scan (**Table 4.1**). In first homologous series with octyloxy chain at chalcone end of the molecules, compound **10a** showed two endothermic transitions on heating cycle associated with Cr-SmC and SmC-Iso at 111.5°C & 127.5°C respectively, while three exothermic transitions during cooling cycle associated with Iso-N, N-SmC and SmC-Cr at 124.1°C, 118.9°C & 76.9°C respectively. Compounds **10b** to **10e** showed enantiotropic liquid crystalline properties with two endothermic transitions during heating cycle related to Cr-SmC and SmC-Iso, while two exothermic transitions during cooling cycle (**Table 4.1, Fig- 4.4a**).

Table 4.1: Mesophase assignments, transition temperature °C of compounds **10a-e** and **14a-e** as determined by POM and DSC.

Compd	n	2 nd heating process ^a		1 st cooling process ^a	
		Temp °C (ΔH KJmol ⁻¹)		Temp °C (ΔH KJmol ⁻¹)	
10a	10	Cr 111.5(-22.83)	SmC 127.5(-1.89) Iso	Iso 124.1(1.99) N 118.9(0.38)	SmC 76.9(16.38) Cr
10b	12	Cr 109.4(-17.85)	SmC 130.7(-2.13) Iso	Iso 123.6(1.91)	SmC 78.2(15.37) Cr
10c	14	Cr 100.0(-44.83)	SmC 135.0(-2.40) Iso	Iso 129.1(3.48)	SmC 81.3(17.08) Cr
10d	16	Cr 104.8(-64.49)	SmC 129.2(-4.06) Iso	Iso 124.2(4.14)	SmC 78.0 (22.81) Cr
10e	18	Cr 93.5(-18.09)	SmC 106.6(-8.15) Iso	Iso 103.6*	SmC 82.2(16.12)Cr
14a	10	Cr 110.1(-33.04)	Iso	Iso 108.9(0.65) N 76.7(14.32)	Cr
14b	12	Cr 121.2(-54.81)	Iso	Iso 115.7(68.13) N 81.6(18.95)	Cr
14c	14	Cr 110.4(-27.81) N 117.7(-1.24)	Iso	Iso 114.3(2.05) N 91.2(29.78)	Cr
14d	16	Cr 109.1(-25.40) SmA 117.4(-1.28)	Iso	Iso 114.3(2.26) SmA 90.3(30.55)	Cr
14e	18	Cr 113.1(-35.24) SmA 120.30(2.05)	Iso	Iso 117.2(2.68) SmA 98.8(40.85)	Cr

^a Cr: Crystalline state; N: Nematic; SmA: Smectic A; SmC: Smectic C; Iso: Isotropic state;

*Mesophase transition temperature observed in POM study

In second homologous series, the variation of alkoxy group at chalcone terminal of the molecules, compounds **14a-b** showed only endotherms for Cr-Iso transitions at 110.1°C & 121.2°C respectively on heating cycle, while two exotherms associated with Iso-N & N-Cr during cooling cycle (**Table 4.1 & Fig- 4.4b**). Compound **14c-e** exhibited enantiotropic liquid crystalline properties. Compound **14c** showed two endotherms 110.4°C for Cr-N & 117.7°C for N-Iso transitions respectively and two exotherms 114.3°C for Iso-N & 91.2°C for N-Cr transitions. Compound **14d** exhibited two endotherms related to Cr-SmA (109.1°C) and SmA-Iso (117.4°C) while heating and two exotherms associated to Iso-SmA (114.3°C) and SmA-Cr (90.3°C) phase during cooling cycle (**Table 4.1, Fig- 4.4c**).

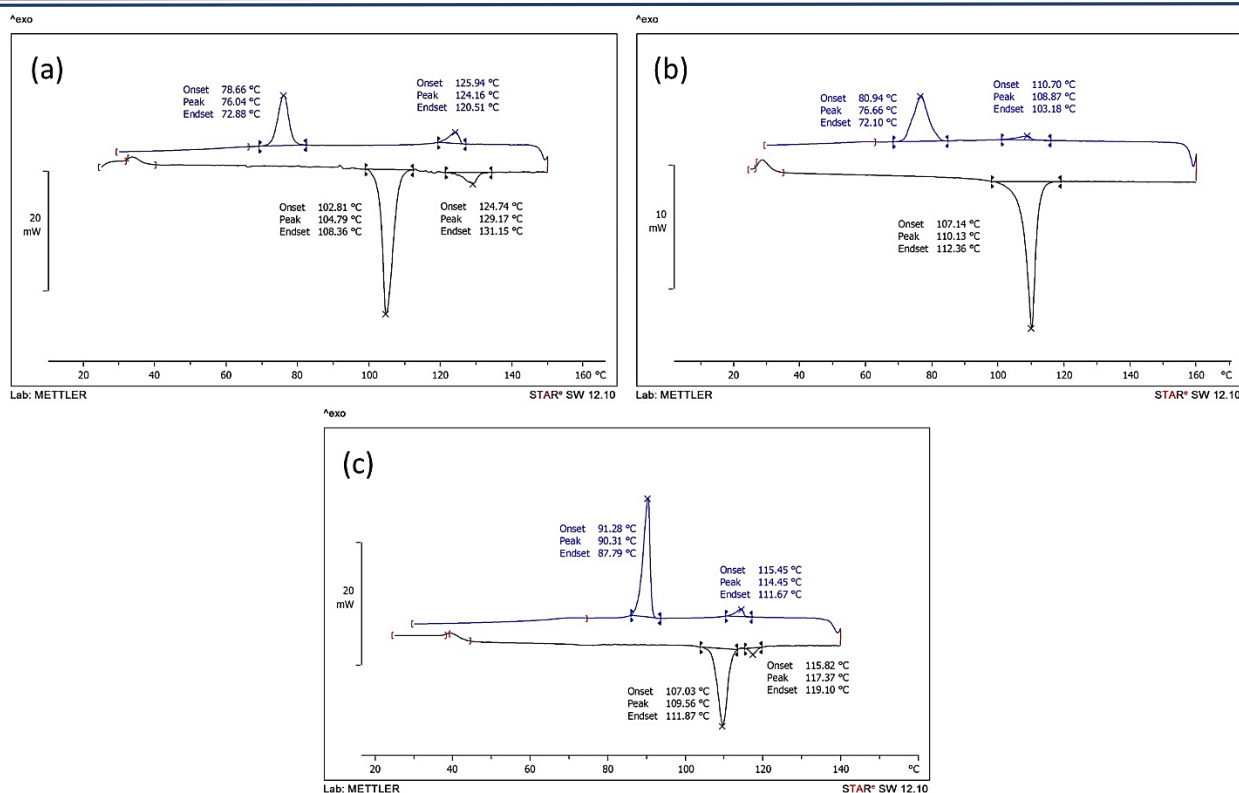


Figure- 4.4 DSC plot in both heating and cooling cycles (at the rate of 10 °C/min.) along with transition temperatures (a) compound **10d** (b) compound **14a** (c) compound **14d**

4.2.2.3 Structure Mesomorphic Relationship:

Further, graph for alkoxy chain length vs the temperature of mesophase transitions were plotted (**Fig- 4.5**). Typical mesophases such as nematic, SmA and SmC phases were observed for newly prepared mesogens. The clearing temperature was increased in both the series with increase in alkoxy chain length and then decreased with the increase of chain length (**Fig- 4.5**). Compounds **14a-e** showed low clearing temperature as compared to that for compounds **10a-e**. Compound **5** has shown both nematic and SmA mesophase transitions. On changing octyloxy to decyloxy chain length on coumarin end of the molecule, it resulted in molecules to show Iso-N and N-SmC mesophase transitions, while higher analogues showed only Iso-SmC transitions due to increase of intermolecular forces with increase chain length to result in layered packing. While, on changing octyloxy with decyloxy chain length on chalcone end of the molecules, it resulted in loss of SmA mesophase transition and exhibited Iso-N phase transition only. Similarly, compounds with dodecyloxy and tetradecyloxy chain length exhibited Iso-N phase transition as a result of change in shape anisotropy as well as less intermolecular interactions between the mesogenic units. While, higher analogues have shown enantiotropic Iso-SmA phase transition.

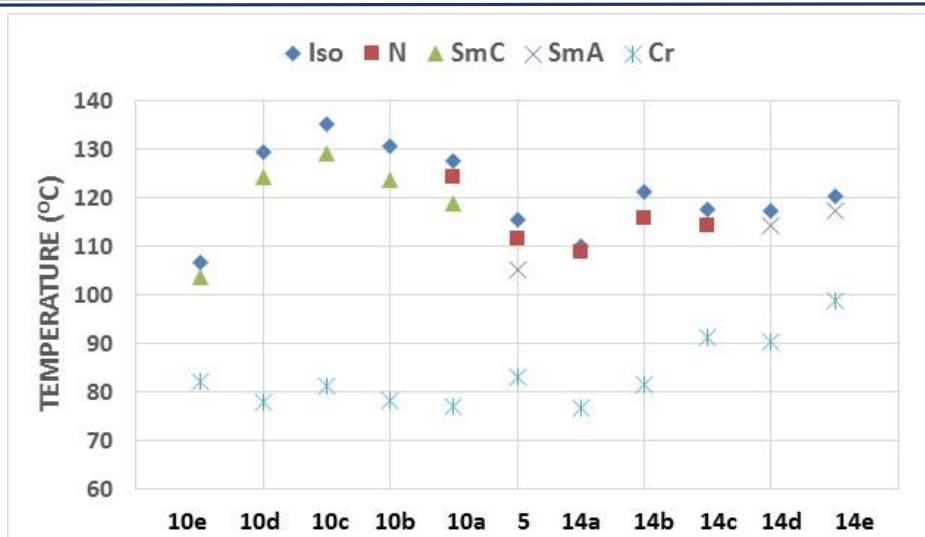


Figure- 4.5 Effect of chain length variation on both end of the molecules on transition temperatures of compounds **5**, **10a-e** and **14a-e**

4.2.2.4 X-ray diffraction studies:

Unsymmetric coumarin chalcone derivatives **10d**, **14a** and **14d** were studied for powder X-ray diffraction analysis to study the identification of mesophase (**Fig- 4.6**). The powder XRD analysis of compound **10d** at 112 °C showed two peaks. First sharp reflection was observed in the small angle regime (layer spacing 36.2 Å) and second broad hump in the wide-angle region (layer spacing 4.4 Å) (**Fig- 4.6a**). Similar set of two peaks were observed for compound **14a**, however sharp reflection peak was found to be with very low intensity when compared with compound **10d** corresponding to more liquid like nature (**Fig- 4.6b**). While compound **14d** showed the sharp reflection peak with layer spacing of 41.6 Å and the broad hump in the wide-angle region (layer spacing 4.3 Å) (**Fig- 4.6c**). The SmA and SmC mesophases can be easily distinguished based on their powder XRD pattern at small-angle region. The peak in small angle region appeared with very low intensity in compound **14a** with nematic mesophase as compared to that in compounds **10d** and **14d**. At the same time diffused broad halo around 4.3-4.4 Å was found to be almost similar for all the compounds as originated as a result of liquid like nature of alkoxy terminal. For compounds **10d** and **14d**, tilt angle was calculated using the formula $\text{tilt angle } \theta = \cos^{-1}(d/L)$, (where L is molecular length was obtained by DFT optimized structure). The tilt angles were found to be 40.0° and 28.5° respectively for compounds **10d** and **14d**, which further confirms tilted SmC mesophase of compound **10d**, while the orthogonal Smectic-A mesophase of **14d**. Bragg's diffraction equation was used to calculate the inter layer distances from the 2θ values.

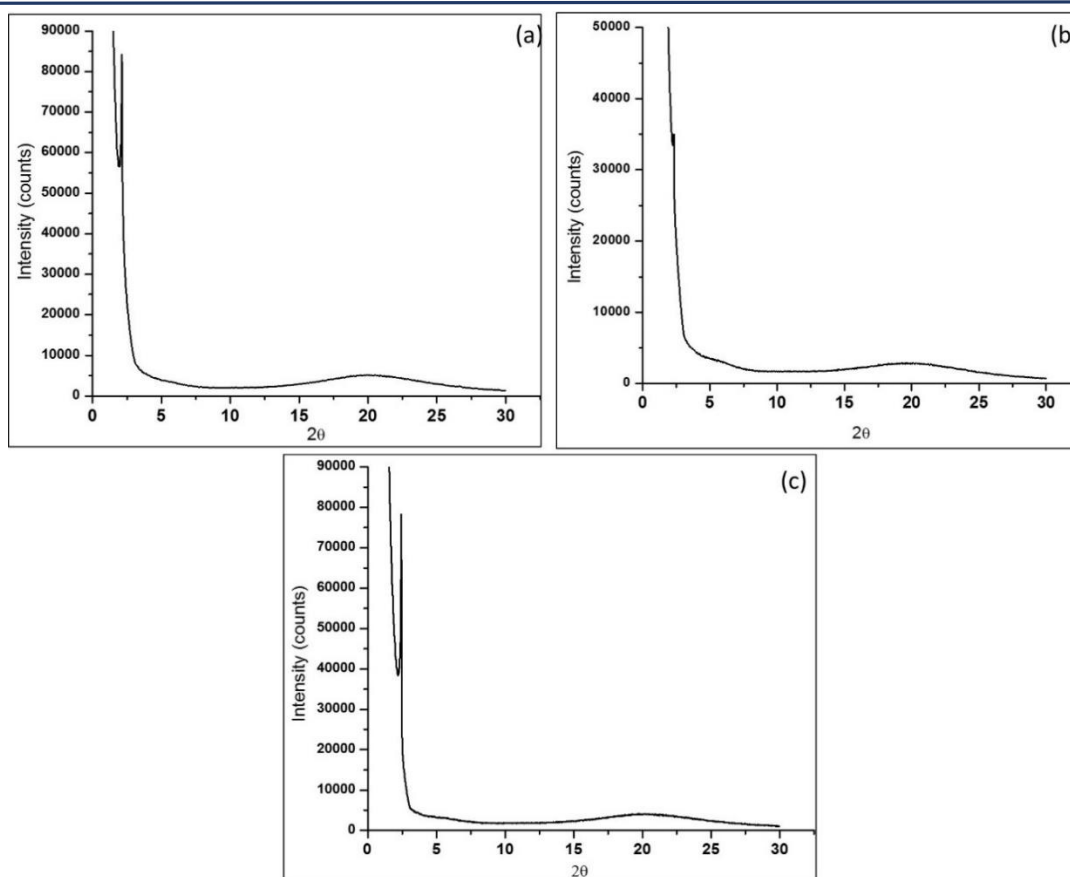


Figure- 4.6 Powder X-ray diffraction analysis at 112 °C (a) compound **10d** (b) compound **14a** and (c) compound **14d** (the scattering intensity (in counts) vs the scattering angle, 2θ)

4.3 DFT calculations:

The DFT calculations were investigated for **10a-e** and **14a-e** in order to develop correlation between the observed mesomorphic properties and theoretical geometrical parameters. All the DFT optimization of compounds were done using B3LYP method at 6-311G (d,p) basis set. All the optimized structures have shown good stability and the frequency for all the compounds were calculated using the same basis set to calculate various parameters. The estimated optimized structures of compounds **10a-e** and **14a-e** are shown in (**Fig- 4.7**).

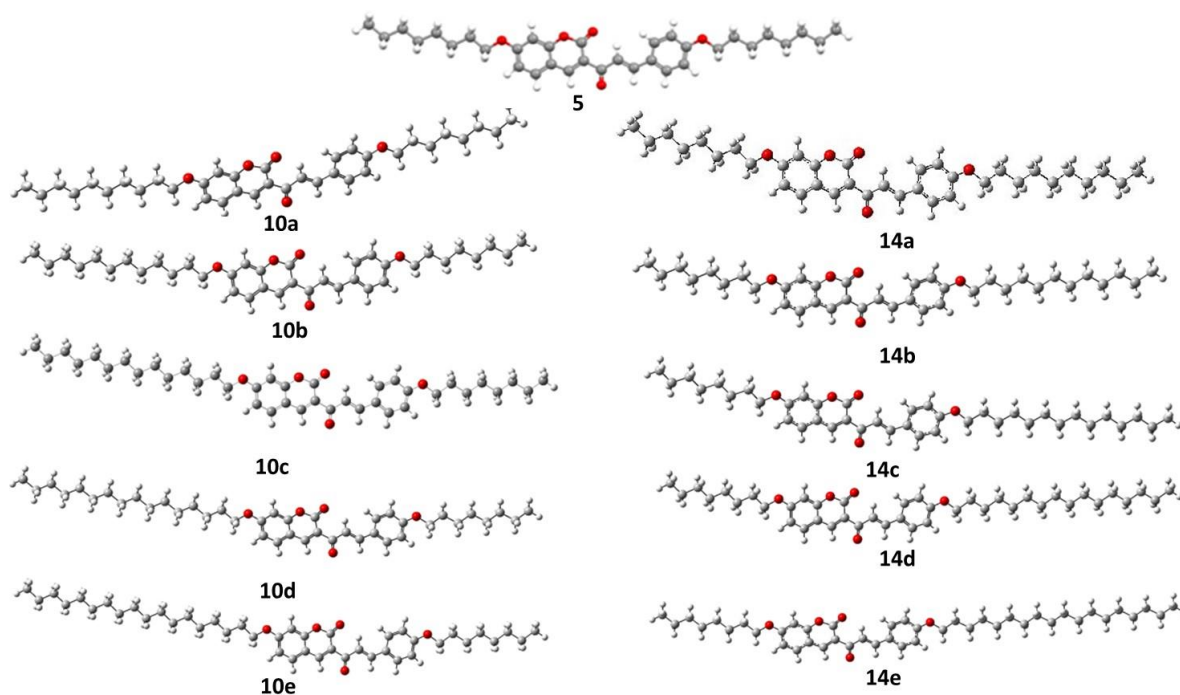


Figure- 4.7 Calculated molecular geometry of the compounds **5**, **10a-e** and **14a-e** (Colour online)

Chalcone derivative **5** was also selected and optimized using same basis set to find a comparative study. All the compounds have shown planar structures (**Fig- 4.7**), which could be one of the factor to align the molecules in parallel pattern to give more ordered mesophase. Compound **5** showed nematic and SmA mesophase. In the first series with octyloxy chain on chalcone end, compounds aspect ratio was increased with increase in alkoxy chain length on coumarin end of the molecule, however clearing temperatures were initially increased (for $n=10,12,14$,) and then decreased (for $n=16,18$). Similar variation of alkoxy chain length on chalcone end of the molecules showed random behavior for clearing temperature with respect to increase in aspect ratio.

4.3.1 Frontier Molecular Orbitals:

The Highest occupied molecular orbital (HOMO), lowest unoccupied molecular orbital (LUMO) and ΔE values of the studied compounds were calculated by the B3LYP/6-311G (d, p) method. The frontier molecular orbitals (FMOs) have been calculated for the compounds **10a-e** and **14a-e** (**Fig- 4.8**) and compared with compound **5**. It was observed that for all the compounds, HOMO are mainly located on chalcone and attached aromatic ring, while LUMO are mainly located on coumarin ring, chalcone group and aromatic ring.

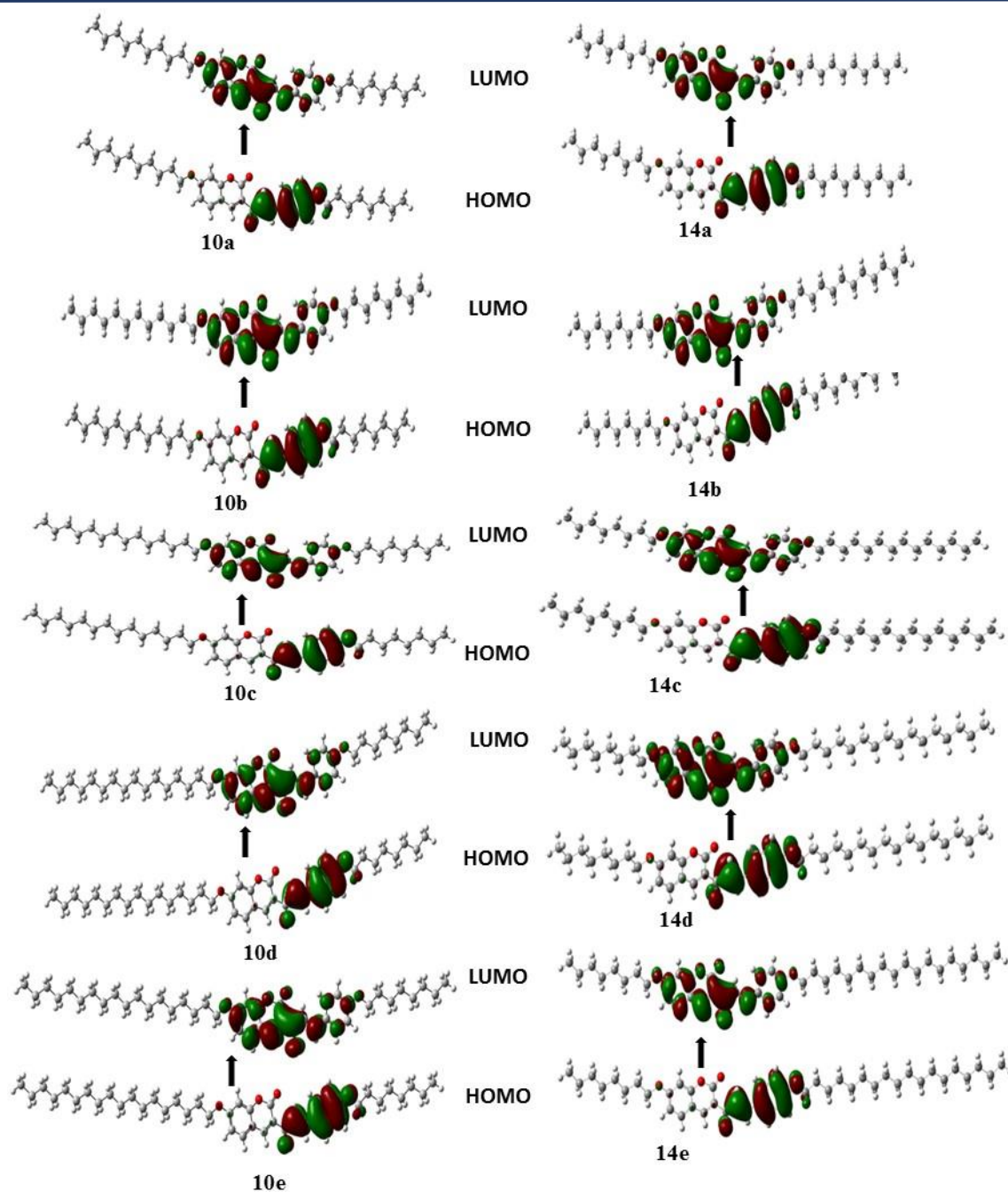


Figure- 4.8 Frontier Molecular orbitals (FMO) (HOMO and LUMO) for compounds **10a-e** and for **14a-e**

Some of the valuable parameters of liquid crystalline compounds can be calculated from energy gap such as global softness and chemical hardness (**Table 4.2**). The ΔE value of molecule can be used to find the chemical reactivity and stability of it. With high ΔE is less polarizable and is generally associated with a low chemical reactivity and high kinetic stability and vice versa [35]. Interestingly the all the studied compounds **5**, **10a-e** and **14a-e**, ΔE values were found to be almost identical (**Table -4.2**). Hence, other parameters such as chemical hardness (η) and

softness (S), electrophilicity index (ω), electronegativity (X) were found to be quite same throughout the variation of terminal alkoxy chain length on both end of the molecules (**Table 4.2**).

Table 4.2: FMO Energies e.V., wavelength of the maximum absorbance softness and other chemical descriptors of the prepared compounds **10a-e** and **14a-e**

Compd	LUMO	HOMO	ΔE	X	η	S	ω	$A = -E_{LUMO}$	$I = -E_{HOMO}$
10a	-2.45	-5.71	3.27	4.08	1.63	16.66	4.90	2.45	5.71
10b	-2.45	-5.71	3.27	4.08	1.63	16.66	4.90	2.45	5.71
10c	-2.45	-5.71	3.27	4.08	1.63	16.66	4.90	2.45	5.71
10d	-2.45	-5.71	3.27	4.08	1.63	16.66	4.90	2.45	5.71
10e	-2.45	-5.71	3.27	4.08	1.63	16.66	4.90	2.45	5.71
14a	-2.45	-5.71	3.27	4.08	1.63	16.66	4.90	2.45	5.71
14b	-2.45	-5.71	3.27	4.08	1.63	16.66	4.90	2.45	5.71
14c	-2.45	-5.71	3.27	4.08	1.63	16.66	4.90	2.45	5.71
14d	-2.45	-5.71	3.27	4.08	1.63	16.66	4.90	2.45	5.71
14e	-2.45	-5.71	3.27	4.08	1.63	16.66	4.90	2.45	5.71

4.3.2 Molecular Electrostatic Potential:

The molecular electrostatic potential (MEP) of molecules can provide overall electron density distribution over the molecules as well as possible molecular interaction which will further affect overall dipole moment and polarizability of molecules [36] (**Table 4.3 and Fig-4.9**). The MEP maps were calculated to locate charge distribution by using the same basis sets (**Fig- 4.9**) to explore the possible intra- and intermolecular interactions sites on the molecule.

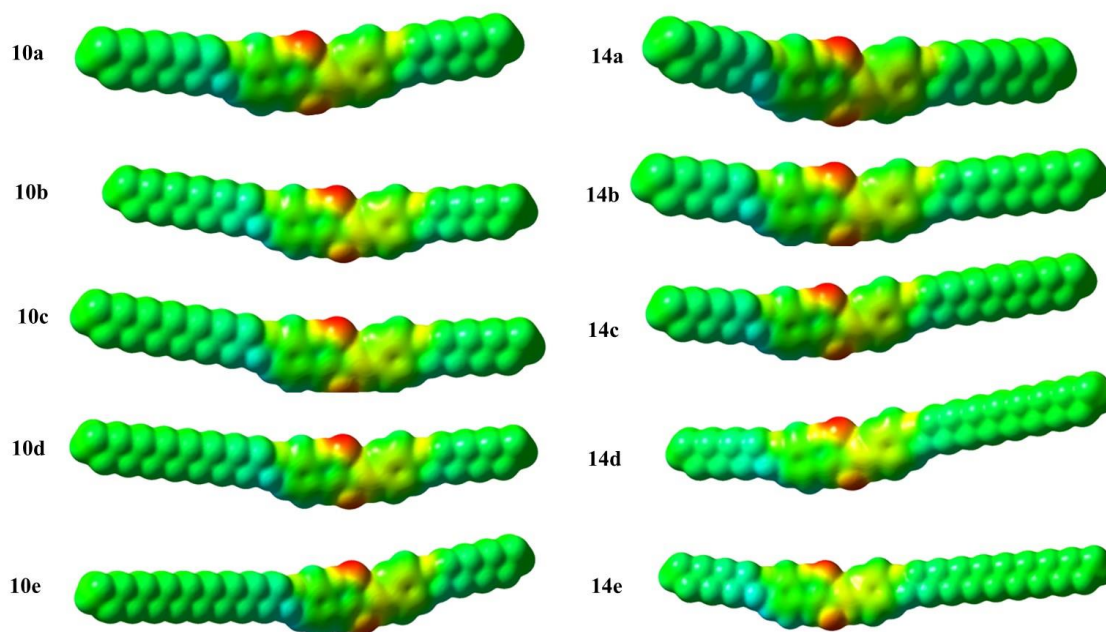


Figure- 4.9 Molecular electrostatic potentials (MEP) for the prepared compounds **10a-10e** and **14a-14e**

HOMO, LUMO and Molecular electrostatic potential (MEP) also optimized and calculated for reference compound **5** and compared with compounds **10d** and **14d**. It was observed the same location for HOMO, LUMO and MEP in comparison study. That is, HOMO's are mainly located on chalcone and attached aromatic ring, while LUMO are mainly located on coumarin ring, chalcone group and aromatic ring. (**Fig 4.10**).

For all the studied compounds, electron deficient centers are mainly localized on chalcone or coumarin part (red color region), while the electron rich regions are located on both terminal alkoxy chains (Blue color region). For compounds **10a-e**, dipole moments as well as polarizability were found to increase with successive variation in alkoxy chain at coumarin end (**Table 4.3**).

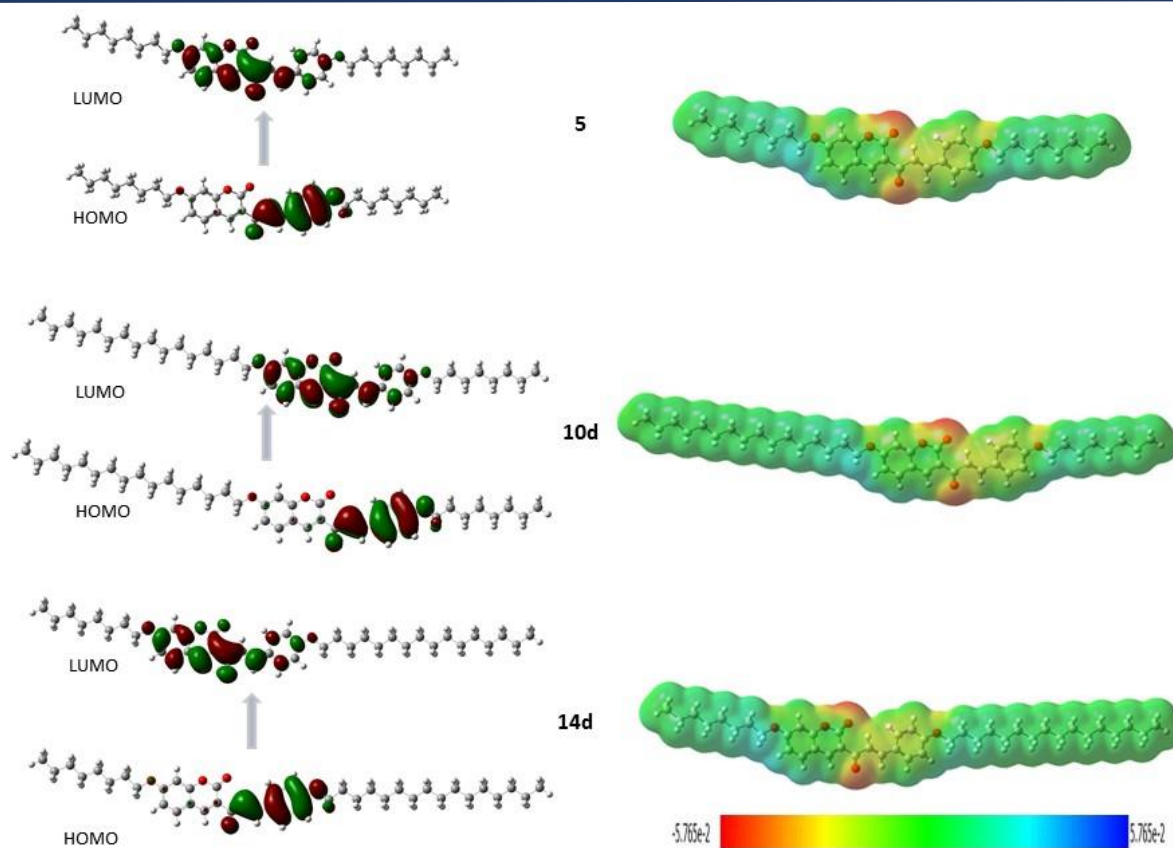


Figure- 4.10 Frontier Molecular orbitals (FMOs) and Molecular electrostatic potentials (MEP) for the prepared compounds **5**, **10d** and **14d**

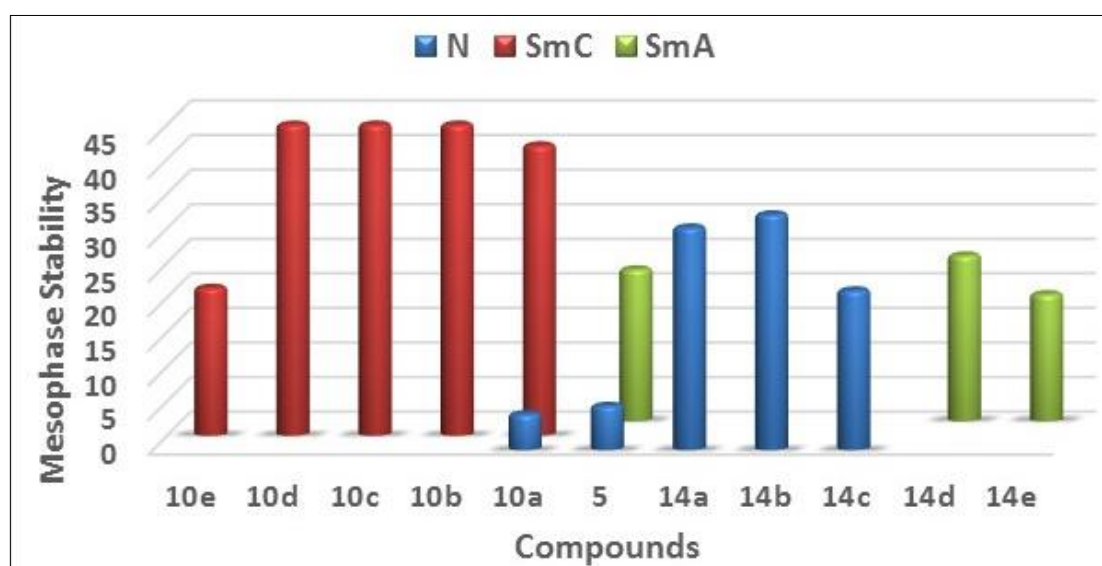
4.3.3 Relation between variations in alkoxy chain length with mesomorphic phases

On varying alkoxy chain length on coumarin ring has resulted in enhancement of the head-tail interaction to give SmC mesophase and overall very good stability was observed on varying alkoxy chain length (**Fig 4.11**). However, on varying alkoxy chain length on chalcone end, dipole moment was decreased on increasing the alkoxy chain length for compounds **14a-d** and again increased for compound **14e**. In this series, compounds **14a-b** exhibited monotropic nematic mesophase, while compound **14c** showed enantiotropic nematic mesophase (**Table 4.3**).

At the same time nematic mesophase stability was initially increased with increase in alkoxy chain on chalcone end and then decreased (**Fig 4.11**). On the other hand, enantiotropic SmA mesophase was observed for compounds **14d-e**. At the same time polarizability was found to be increasing initially for compounds **14a-e** except that it is decreased for compound **14d** with increase in alkoxy chain on chalcone end.

Table 4.3: Mesomorphic parameters in cooling cycle ($^{\circ}\text{C}$), dipole moment (Debye), polarizability α (Bohr^3), aspect ratio of the studied compounds **5**, **10a-e** and **14a-e**

Compd	ΔT_{Cr}	ΔT_{SmA}	ΔT_{SmC}	ΔT_{N}	Dipole moment	Polarizability	Dimension (\AA)		Aspect ratio L/D
							Length L	Width D	
5	28.5	22.0	–	6.4	3.158	518.128	37.062	5.60	6.62
10a	47.2	–	42.0	5.2	3.181	543.335	39.615	5.70	6.95
10b	45.4	–	45.4	–	3.189	568.362	42.164	6.01	7.02
10c	47.8	–	47.8	–	3.208	593.197	44.718	6.26	7.14
10d	46.2	–	46.2	–	3.212	617.997	47.276	6.47	7.31
10e	21.4	–	21.4	–	3.215	642.763	49.834	6.65	7.49
14a	32.2	–	–	32.2	3.141	543.347	39.622	5.74	6.91
14b	34.1	–	–	34.1	3.131	568.321	42.183	5.87	7.19
14c	23.1	–	–	23.1	3.127	593.195	44.742	5.99	7.47
14d	24.0	24.0	–	–	2.948	565.386	47.304	6.10	7.75
14e	18.4	18.4	–	–	3.121	642.834	49.866	6.22	8.02

**Figure- 4.11** The relation between the variation of chain length in compounds and N, SmC and SmA mesophase range

4.4 Conclusion

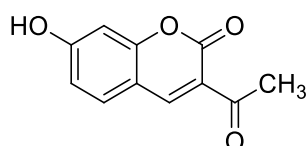
Unsymmetric Coumarin chalcone derivatives were designed with various alkoxy chain at both terminal ends of the molecule. All the compounds **10a-e** and **14a-e** were synthesized and fully characterized. In the first homologous series with octyloxy chain on chalcone end, compounds were prepared with varied alkoxy chain on coumarin terminal of the molecule. Compound **10a** has shown SmC and Nematic phases while compounds **10b-e** have shown enantiotropic stable SmC mesophase. In the second series with octyloxy chain on coumarin end, compounds were prepared with varied alkoxy chain on chalcone terminal of the molecule. In this particular series, compounds **14a-c** have shown monotropic nematic mesophases, while compound **14d-e** have shown enantiotropic SmA mesophases. Types of mesophases were also confirmed from the powder X-ray diffraction analysis at 112°C and diffraction patterns were found to be in close agreement to those identified by using POM. To understand this difference between the assembling behaviors of molecules with variation of terminal alkoxy chain in both the series, the geometrical and electronic parameters were calculated from the optimized DFT structures and compared with compound **5**. For both the series, parameters such as band gap, chemical hardness and softness were found to be almost unchanged. While dipole moments and polarizability were found to be affected by variation of alkoxy chain length at both ends of the molecules. Variation of alkoxy chain length at chalcone end of the molecules have shown effect on dipole moment and total polarizability, which was also observed in mesomorphic behavior in the series.

4.5 Experimental

4.5.1 Materials and Methods

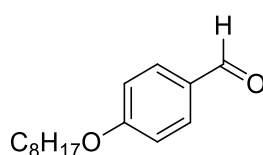
All the chemicals and solvents were purchased from commercial supplier and used after purification. For thin-layer chromatography analysis, silica gel F254 plates (Merck & Co., Kenilworth, NJ, USA) were used. Avra's silica gel (60-120 mesh) was used for column chromatographic purification. All the reactions were carried out in normal atmosphere. Melting points (M.P.) were measured in open capillary tubes and were uncorrected. IR spectra were recorded as KBr pellets on Bruker spectrometer. $^1\text{H-NMR}$ and $^{13}\text{C-NMR}$ spectral data were recorded on Avance Bruker Neo 400 spectrometer (400 MHz) with CDCl_3 or DMSO-d_6 as solvent and J values in Hz. Liquid crystalline properties were studied using Polarizing Optical Microscope (POM) LEICA DM 2500P (Wien, Austria) attached with CAMERA-LEICA-DFC 295 and Heating Pod- LINKA 19. The textures of the compounds were observed by using polarized light with a crossed polarizer at angle of 45 degrees and 10x magnification with the sample in thin film sandwiched between a glass slide and cover. Differential scanning calorimetry (DSC) analysis were carried out during heating and cooling cycles at the rate of $10.0\text{ }^\circ\text{C}/\text{min}$ by using DSC-822, Mettler Toledo (Greifensee, Switzerland) having STARE software.

Synthesis of 3-acetyl,7-hydroxy chromen-2-one (7)



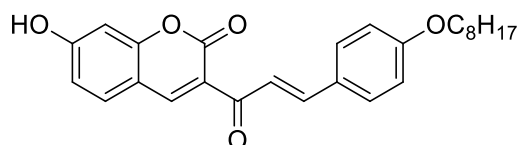
To a solution of 2,4-dihydroxy benzaldehyde (15g, 0.108mol, 1.0 eq) in ethanol (50 mL) was added ethyl acetoacetate (13.62ml, 0.108mol, 1.0 eq) followed by catalytic amount of piperidine (0.1 mL). The resulting mixture was refluxed for 18 h. The completion of reaction was checked by TLC. After completion of reaction, reaction mixture was allowed to cool down to room temperature and concentrated on a rotavapor. The viscous liquid obtained was poured into ice cold water to give solid. The solid obtained was filtered, washed with water, dried and recrystallized from ethanol to give compound **7** as green crystals. Yield: 95%; M.P: 236-238 $^\circ\text{C}$ (Lit [22] M.P. 240 $^\circ\text{C}$)

Synthesis of 4-(octyloxy)benzaldehyde (8)



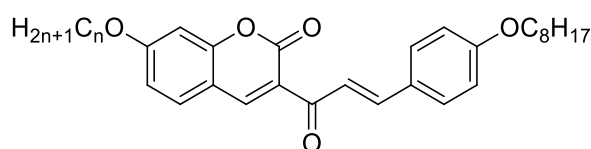
To a solution of 4-hydroxy benzaldehyde **8** (1.0 eq) in DMF (20 mL) was added anhydrous K_2CO_3 (2.5 eq) and stirred at room temperature for 10-15 min. To this mixture, octyl bromide (1.0 mmol) was added and resulting solution was stirred at room temperature for 16-18 h. The completion of reaction was checked by TLC. After completion of reaction, the reaction mixture was poured into ice-cold water. The crude compound was obtained as colorless oil; compound was directly used for next step. Yield: 70-85%.

(E)-7-hydroxy-3-(3-(4-(octyloxy)phenyl)acryloyl)-2H-chromen-2-one (9)



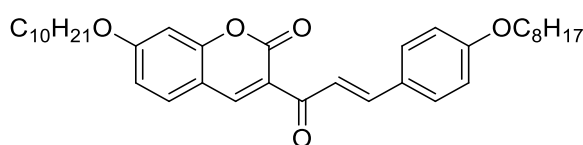
To a solution of 3-acetyl-7-hydroxy coumarin **7** (5.0 g, 24.50 mmol, 1.0 eq) in ethanol (15 ml), 4-octyloxy benzaldehyde **8** (6.30 g, 26.96 mmol, 1.1 eq) was added followed by catalytic amount (3-4 drops) of pyrrolidine and acetic acid. The reaction mixture was refluxed at 78-80 °C for 36 hrs. The progress of reaction was monitored by TLC. The reaction mixture was cooled to room temperature and solvent were evaporated on rotavapor. The residue was poured into ice cold water to give crude product. The crude product was filtered, washed with water, and dried. The crude product was purified by column chromatography using pet ether:ethyl acetate (9:1 to 6:4) to give pure compound 82% Yield, M.P.: 168-170°C; ESI-MS: 421.2 [M+H]⁺.

Synthesis of alkoxy chromen-2-one chalcone derivatives 10a-e



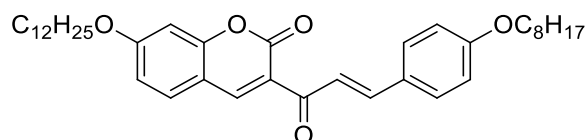
To a solution of compound **9** (200 mg, 0.476 mmol, 1.0 eq) in DMF (15 mL) was added anhydrous K_2CO_3 (262 mg, 1.90 mmol, 4.0 eq), n-alkyl bromide (2.0 eq) and pinch of KI. The resulting mixture was heated at 70-72 °C for 14-16 hours and monitored by TLC. On completion of reaction, reaction mixture was cooled to room temperature and poured into ice cold water to give crude product. The crude product was filtered, dried and recrystallized from ethanol to give pure compound as a yellow solid.

(E)-7-(decyloxy)-3-(3-(4-(octyloxy)phenyl)acryloyl)-2H-chromen-2-one (10a)



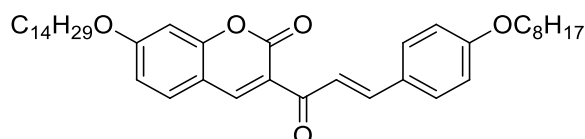
Yield :88%; M.P.: 128-130°C; IR (KBr): 2923, 2853, 1731, 1654, 1599, 1564, 1510, 1472, 1422, 1395, 1342, 1303, 1265, 1185, 1168, 1144, 1072, 1011, 986, 953, 850, 832, 803, 775, 721, 640 cm^{-1} ; $^1\text{H-NMR}$ (400 MHz, CDCl_3) : δ ppm 0.90-0.92 (m, 6H), 1.29-1.36 (m, 20H), 1.46-1.47 (m, 4H), 1.77-1.87 (m, 4H), 4.00 (t, $J = 6.4\text{Hz}$, 2H), 4.06 (t, $J = 6.4\text{Hz}$, 2H), 6.84-6.93 (m, 4H), 7.55 (d, $J = 8.8\text{Hz}$, 1H), 7.63 (d, $J = 8.8\text{Hz}$, 2H), 7.84 (d, $J = 16.0\text{Hz}$, 1H), 7.92 (d, $J = 16.0\text{Hz}$, 1H), 8.59 (s, 1H); $^{13}\text{C-NMR}$ (100 MHz, CDCl_3) : δ ppm 14.14, 14.15, 22.68, 22.70, 25.93, 26.02, 28.90, 29.17, 29.25, 29.33, 29.36, 29.55, 31.82, 31.90, 68.17, 69.01, 100.68, 112.26, 114.18, 114.82, 121.34, 121.68, 127.54, 130.74, 131.22, 144.61, 148.38, 157.63, 159.95, 161.45, 164.68, 186.29; ESI-MS: 561.4 $[\text{M}+\text{H}]^+$; Anal. Calc. for $\text{C}_{36}\text{H}_{48}\text{O}_5$; C, 77.11; H, 8.63; found: C, 77.23; H, 8.71 %.

(E)-7-(dodecyloxy)-3-(3-(4-(octyloxy)phenyl)acryloyl)-2H-chromen-2-one (10b)



Yield : 86%; Melting Point : 132-134°C; IR (KBr): 2922, 2852, 1730, 1655, 1598, 1563, 1509, 1471, 1439, 1421, 1394, 1343, 1303, 1265, 1184, 1168, 1143, 1071, 1022, 985, 952, 850, 832, 776, 756, 721, 679 cm^{-1} ; $^1\text{H-NMR}$ (400 MHz, CDCl_3): δ ppm 0.88-0.91 (m, 6H), 1.28-1.33 (m, 24H), 1.47 (m, 4H), 1.77-1.88 (m, 4H), 4.00 (t, $J = 6.4\text{Hz}$, 2H), 4.05 (t, $J = 6.4\text{Hz}$, 2H), 6.84 (d, $J = 2.0\text{Hz}$, 1H), 6.87-6.93 (m, 3H), 7.55 (d, $J = 8.8\text{Hz}$, 1H), 7.63 (d, $J = 8.8\text{Hz}$, 2H), 7.84 (d, $J = 15.6\text{Hz}$, 1H), 7.92 (d, $J = 15.6\text{Hz}$, 1H), 8.58 (s, 1H); $^{13}\text{C-NMR}$ (100 MHz, CDCl_3) : δ ppm: 14.14, 14.16, 22.68, 22.72, 25.93, 26.02, 28.90, 29.17, 29.25, 29.34, 29.37, 29.55, 29.60, 29.65, 29.67, 31.83, 31.93, 98.17, 69.00, 100.68, 112.26, 114.17, 114.82, 121.34, 121.68, 127.54, 130.74, 131.22, 144.60, 148.38, 157.63, 159.95, 161.45, 164.68, 186.28; ESI-MS 587.30 $[\text{M}-\text{H}]^+$; Anal. Calc. for $\text{C}_{38}\text{H}_{52}\text{O}_5$; C, 77.51; H, 8.90; found: C, 77.56; H, 8.96%.

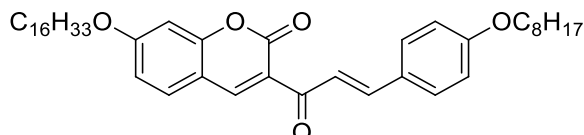
(E)-3-(3-(4-(octyloxy)phenyl)acryloyl)-7-(tetradecyloxy)-2H-chromen-2-one (10c)



Yield : 87%; Melting Point: 136-138°C; IR (KBr): 2924, 2850, 1722, 1652, 1617, 1595, 1562, 1510, 1469, 1433, 1367, 1342, 1293, 1266, 1249, 1162, 1069, 1038, 1019, 994, 868, 841, 806, 775, 753, 723, 641 cm^{-1} ; $^1\text{H-NMR}$ (400 MHz, CDCl_3) : δ ppm 0.87-0.90 (m, 6H), 1.27-1.33 (m, 28H), 1.47 (m, 4H), 1.77-1.82 (m, 4H), 3.99 (t, $J = 6.4\text{Hz}$, 2H), 4.05 (t, $J = 6.0\text{Hz}$, 2H),

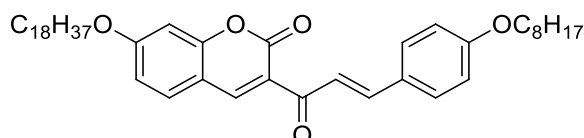
6.82-6.92 (m, 4H), 7.54 (d, $J = 8.4\text{Hz}$, 1H), 7.63 (d, $J = 8.4\text{Hz}$, 2H), 7.83 (d, $J = 16\text{Hz}$, 1H), 7.91 (d, $J = 16\text{Hz}$, 1H), 8.58 (s, 1H); $^{13}\text{C-NMR}$ (100 MHz, CDCl_3) : δ ppm 14.14, 14.16, 22.68, 22.72, 25.94, 26.02, 28.90, 29.17, 29.26, 29.34, 29.36, 29.39, 29.56, 29.60, 29.68, 29.70, 29.71, 31.83, 31.95, 68.17, 69.00, 100.67, 112.26, 114.16, 114.82, 121.32, 121.68, 127.54, 130.74, 131.21, 144.59, 148.37, 157.63, 159.94, 161.45, 164.68, 186.25; ESI-MS: 617.6 $[\text{M}+\text{H}]^+$; Anal. Calc. for $\text{C}_{40}\text{H}_{56}\text{O}_5$; C, 77.88; H, 9.15; found: C, 77.93; H, 9.21%.

(E)-7-(hexadecyloxy)-3-(3-(4-(octyloxy)phenyl)acryloyl)-2H-chromen-2-one (10d)

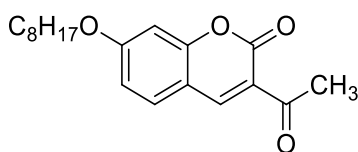


Yield 86%; Melting Point: 132-134°C; IR (KBr): 2950, 2923, 2849, 1721, 1651, 1617, 1594, 1561, 1509, 1468, 1431, 1367, 1342, 1293, 1266, 1249, 1162, 1068, 1023, 994, 870, 841, 804, 775, 753, 722, 641 cm^{-1} ; $^1\text{H-NMR}$ (400 MHz CDCl_3): δ ppm 0.87-0.90 (m, 6H), 1.27-1.32 (m, 32H), 1.45-1.46 (m, 4H), 1.78-1.85 (m, 4H), 3.99 (t, $J = 6.4\text{Hz}$, 2H), 4.04 (t, $J = 6.4\text{Hz}$, 2H), 6.83 (d, $J = 2.0\text{Hz}$, 1H), 6.88-6.92 (m, 3H), 7.55 (d, $J = 8.8\text{Hz}$, 1H), 7.63 (d, $J = 8.8\text{Hz}$, 2H), 7.84 (d, $J = 15.6\text{Hz}$, 1H), 7.92 (d, $J = 15.6\text{Hz}$, 1H), 8.58 (s, 1H); $^{13}\text{C-NMR}$ (100 MHz CDCl_3) : δ ppm: 14.14, 14.16, 22.68, 22.72, 25.94, 26.02, 28.90, 29.17, 29.25, 29.36, 29.39, 29.56, 29.61, 29.68, 29.72, 31.83, 31.95, 68.16, 69.00, 100.66, 112.25, 114.15, 114.81, 121.31, 121.67, 127.54, 130.73, 131.21, 144.58, 148.36, 157.62, 159.93, 161.45, 164.67, 186.23; ESI-MS 645.8 $[\text{M}+\text{H}]^+$; Anal. Calc. for $\text{C}_{42}\text{H}_{60}\text{O}_5$; C, 78.22; H, 9.38; found: C, 78.26; H, 9.45%.

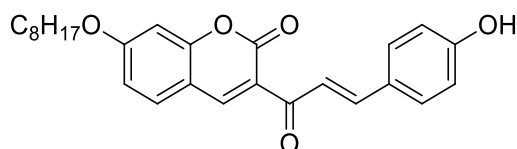
(E)-7-(octadecyloxy)-3-(3-(4-(octyloxy)phenyl)acryloyl)-2H-chromen-2-one (10e)



Yield 88%; Melting Point: 110-112°C; IR (KBr): 2920, 2851, 1720, 1653, 1616, 1596, 1563, 1509, 1470, 1435, 1342, 1293, 1266, 1250, 1162, 1069, 1023, 993, 870, 841, 805, 775, 721, 641 cm^{-1} ; $^1\text{H-NMR}$ (400 MHz, CDCl_3) : δ ppm 0.87-0.90 (m, 6H), 1.26-1.32 (m, 36H), 1.46-1.47 (m, 4H), 1.77-1.86 (m, 4H), 4.00 (t, $J = 6.8\text{Hz}$, 2H), 4.05 (t, $J = 6.4\text{Hz}$, 2H), 6.83 (d, $J = 2.0\text{Hz}$, 1H), 6.89-6.93 (m, 4H), 7.56 (d, $J = 8.4\text{Hz}$, 1H), 7.63 (d, $J = 8.8\text{Hz}$, 2H), 7.84 (d, $J = 15.6\text{Hz}$, 1H), 7.92 (d, $J = 15.6\text{Hz}$, 1H), 8.59 (s, 1H); $^{13}\text{C-NMR}$ (100 MHz, CDCl_3): δ ppm 14.14, 14.16, 22.68, 22.72, 25.94, 26.20, 28.90, 29.17, 29.25, 29.36, 29.39, 29.47, 29.56, 29.60, 29.69, 29.72, 31.82, 31.95, 68.17, 69.01, 100.67, 112.25, 114.17, 114.82, 121.32, 121.68, 127.53, 130.73, 131.22, 144.60, 148.37, 157.62, 159.94, 161.45, 164.69, 186.27; ESI-MS: 673.9 $[\text{M}+\text{H}]^+$; Anal. Calc. for $\text{C}_{44}\text{H}_{64}\text{O}_5$; C, 78.53; H, 9.59; found: C, 78.59; H, 9.64%.

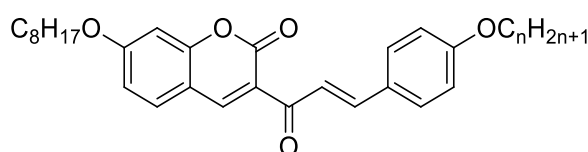
Synthesis of 3-acetyl-7-(octyloxy)-2H-chromen-2-one (11)

To a solution of 3-acetyl-7-hydroxy coumarin **7** (5.0 g, 24.48 mmol, 1.0 eq) in DMF (50ml) was added anhydrous K_2CO_3 (5.06 g, 36.72 mmol, 1.5 eq) followed by octyl bromide (4.67 ml, 26.92 mmol, 1.1 eq) and pinch of KI. The resulting mixture was heated at 70-72 °C for 14-16 hours and was monitored by TLC. The reaction mixture was cooled to room temperature and poured into ice-cold water to give crude compound. The crude compound was filtered, dried and recrystallized from ethanol to give compound **11**. Yield: 72%, M.P. 110-112°C.

Synthesis of (E)-3-(3-(4-hydroxyphenyl)acryloyl)-7-(octyloxy)-2H-chromen-2-one (13)

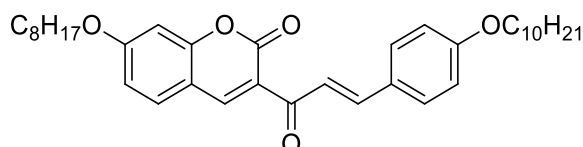
To **11** in ethanol was added 4-hydroxy benzaldehyde **12** along with small amount of pyrrolidine and acetic acid. The reaction mixture was heated for 48 hrs. The completion of reaction was checked by TLC. The reaction mixture was cooled to room temperature and solvent was evaporated on rotavapor, then poured into ice. The product obtained was filtered, washed with cold water and dried. The crude product was purified by column chromatography using pet ether: ethyl acetate (9:1 to 6:4) to give pure compound **13** as a yellow solid.

Yield : 72%; M.P.: 148-150°C; IR (KBr): 3289, 3043, 2916, 2852, 1700, 1653, 1593, 1570, 1513, 1447, 1376, 1357, 1277, 1247, 1193, 1166, 1084, 1019, 997, 827, 778, 754, 713, 649, 595, 570, 529 cm^{-1} ; 1H -NMR (400 MHz, $CDCl_3$): δ ppm 0.86 (t, $J = 6.4Hz$, 3H), 1.25-1.28 (m, 8H), 1.37-1.40 (m, 2H), 1.71-1.75 (m, 2H), 4.10 (t, 6.4Hz, 2H), 6.84 (d, $J = 8.8Hz$, 2H), 7.00 (dd, $J = 8.8Hz$ & 2.4Hz, 1H), 7.06 (d, $J = 2.4Hz$, 1H), 7.58-7.66 (m, 4H), 7.84 (d, 8.8Hz, 1H), 8.65 (s, 1H), 10.17 (s, 1H); ^{13}C -NMR (400 MHz, $CDCl_3$): δ ppm 14.45, 22.56, 25.87, 28.83, 29.14, 29.16, 31.71, 39.30, 39.51, 39.72, 39.93, 40.14, 40.35, 40.55, 69.11, 101.10, 112.43, 114.21, 116.44, 121.61, 121.80, 126.08, 131.27, 132.29, 144.44, 148.08, 157.35, 159.43, 160.76, 164.49, 186.63; ESI-MS: 421.2[M+H] $^+$.

Synthesis of (E)-3-(3-(4-n-alkoxyphenyl)acryloyl)-7-(octyloxy)-2H-chromen-2-one 14a-e:

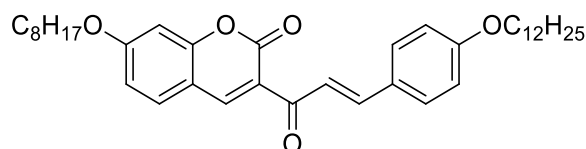
To a solution of compound **13** (200 mg, 0.476 mmol, 1.0 eq) in DMF (10 mL) was added anhydrous K_2CO_3 (1.5 eq) followed by alkyl bromide (1.1 eq) and pinch of KI. The reaction mixture was heated at 70-72 °C for 16-18 hrs and monitored by TLC. On completion of the reaction, mixture was cooled to room temperature and poured into ice cold water to give crude product. The crude product was filtered, dried and recrystallized from ethanol to give compound as a yellow solid.

(E)-3-(3-(4-(decyloxy)phenyl)acryloyl)-7-(octyloxy)-2H-chromen-2-one (14a)



Yield : 82.70%; M.P.: 110-112°C; IR (KBr): 2922, 2850, 1725, 1654, 1597, 1568, 1546, 1506, 1467, 1426, 1377, 1356, 1289, 1250, 1211, 1168, 1117, 1063, 1015, 984, 957, 905, 841, 822, 775, 721, 642, 593, 574 cm^{-1} ; 1H -NMR (400 MHz, $CDCl_3$) : δ ppm 0.91-0.93 (m, 6H), 1.29-1.37 (m, 20H), 1.44-1.51 (m, 4H), 1.78-1.88 (m, 4H), 4.01 (t, $J = 6.8Hz$, 2H), 4.07 (t, $J = 6.4Hz$, 2H), 6.85 (d, $J = 2.0Hz$, 1H), 6.85-6.94 (m, 3H), 7.57 (d, $J = 8.8Hz$, 1H), 7.65 (d, $J = 8.8Hz$, 2H), 7.85 (d, $J = 16.0Hz$, 1H), 7.93 (d, $J = 16.0Hz$, 1H), 8.60 (s, 1H); ^{13}C -NMR (100 MHz, $CDCl_3$) : δ ppm 14.14, 14.16, 22.67, 22.71, 25.94, 26.02, 28.90, 29.17, 29.22, 29.30, 29.34, 29.40, 29.58, 31.80, 31.91, 68.18, 69.01, 100.68, 112.26, 114.19, 114.83, 121.34, 121.68, 127.54, 130.75, 131.22, 144.64, 148.40, 157.63, 159.97, 161.46, 164.69, 186.31; ESI-MS: 561.4 $[M+H]^+$; Anal. Calc. for $C_{36}H_{48}O_5$; C, 77.11; H, 8.63; found: C, 77.27; H, 8.69%.

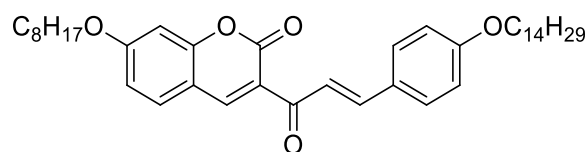
(E)-3-(3-(4-(dodecyloxy)phenyl)acryloyl)-7-(octyloxy)-2H-chromen-2-one (14b)



Yield : 80.71%; Melting Point : 122-124°C; IR (KBr): 2919, 2851, 1725, 1654, 1598, 1569, 1545, 1507, 1469, 1426, 1377, 1356, 1288, 1252, 1209, 1168, 1117, 1063, 1003, 955, 844, 776, 723, 642, 592, 570 cm^{-1} ; 1H -NMR (400 MHz, $CDCl_3$) : δ ppm 0.88-0.91 (m, 6H), 1.26-1.33 (m, 24H), 1.45-1.47 (m, 4H), 1.77-1.84 (m, 4H), 4.01 (t, $J = 6.4Hz$, 2H), 4.07 (t, $J = 6.4Hz$, 2H), 6.82 (d, $J = 2.0Hz$, 1H), 6.88-6.92 (m, 3H), 7.55 (d, $J = 8.8 Hz$, 1H), 7.62 (d, $J = 8.8Hz$, 2H), 7.83 (d, $J = 16Hz$, 1H), 7.90 (d, $J = 16Hz$, 1H), 8.58 (s, 1H); ^{13}C -NMR (100 MHz, $CDCl_3$) : δ ppm 14.14, 14.16, 22.67, 22.72, 25.94, 26.02, 28.90, 29.17, 29.22, 29.30, 29.38, 29.40, 29.59, 29.61, 29.66, 29.68, 31.80, 68.18, 69.01, 100.68, 112.27, 114.19, 114.83, 121.36, 121.68,

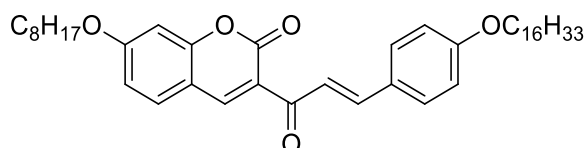
127.54, 130.75, 131.22, 144.64, 148.40, 157.64, 159.97, 161.46, 164.69, 186.32; ESI-MS: 587.30[M-H]⁺; Anal. Calc. for C₃₈H₅₂O₅; C, 77.51; H, 8.90; found: C, 77.59; H, 8.93%

(E)-3-(3-(4-(octyloxy)phenyl)acryloyl)-7-(tetradecyloxy)-2H-chromen-2-one (14c)



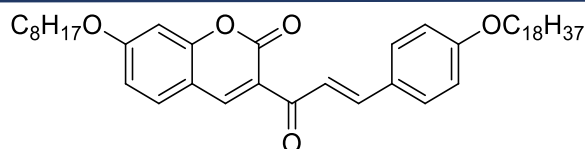
Yield : 87.57%; Melting Point : 118-120 °C; IR (KBr) : 2921, 2852, 2312, 1718, 1658, 1607, 1562, 1509, 1471, 1339, 1302, 1262, 1164, 1142, 1079, 1033, 1008, 975, 854, 830, 723, 639, 570cm⁻¹; ¹H-NMR (400 MHz, CDCl₃) : δ ppm 0.88-0.93 (m, 6H), 1.28-1.37 (m, 28H), 1.47 (t, *J* = 7.2Hz, 4H), 1.79-1.87 (m, 4H), 4.01 (t, *J* = 6.4Hz, 2H), 4.07 (t, *J* = 6.4Hz, 2H), 6.84 (d, *J* = 2.0Hz, 1H), 6.85-6.94 (m, 3H), 7.56 (d, *J* = 8.8Hz, 1H), 7.64 (d, *J* = 8.8Hz, 2H), 7.85 (d, *J* = 15.6Hz, 1H), 7.93 (d, *J* = 15.6Hz, 1H), 8.60 (s, 1H); ¹³C-NMR (100 MHz, CDCl₃) : δ ppm 14.13, 14.16, 22.67, 22.72, 25.94, 26.02, 28.90, 29.17, 29.21, 29.29, 29.39, 29.59, 29.62, 29.68, 29.71, 31.80, 31.94, 68.18, 69.01, 100.69, 112.27, 114.18, 114.83, 121.36, 121.69, 127.54, 130.57, 131.22, 144.62, 148.38, 157.64, 159.96, 161.46, 164.69, 186.31; ESI-MS 617.6 [M+H]⁺; Anal. Calc. for C₄₀H₅₆O₅; C, 77.88; H, 9.15; found: C, 77.96; H, 9.23%.

(E)-3-(3-(4-(hexadecyloxy)phenyl)acryloyl)-7-(octyloxy)-2H-chromen-2-one (14d)



Yield : 84.96%; Melting Point : 118-120°C; IR (KBr): 2921, 2849, 1713, 1655, 1596, 1565, 1542, 1507, 1470, 1427, 1342, 1305, 1263, 1163, 1140, 1068, 1016, 983, 842, 811, 753, 720, 640, 572 cm⁻¹; ¹H-NMR (400 MHz CDCl₃) : δ ppm 0.88-0.91 (m, 6H), 1.27-1.31 (m, 32H), 1.43-1.49 (m, 4H), 1.79-1.88 (m, 4H), 4.00 (t, *J* = 6.8Hz, 2H), 4.06 (t, *J* = 6.4Hz, 2H), 6.84 (d, *J* = 1.6Hz, 1H), 6.85-6.94 (m, 3H), 7.56 (d, *J* = 8.8Hz, 1H), 7.64 (d, *J* = 8.8Hz, 2H), 7.89 (d, *J* = 16.4Hz, 1H), 7.95 (d, *J* = 16.4Hz, 1H), 8.60 (s, 1H); ¹³C-NMR (100 MHz, CDCl₃) : δ ppm 14.14, 14.17, 22.67, 22.72, 25.94, 26.02, 28.90, 29.17, 29.22, 29.30, 29.40, 29.59, 29.62, 29.69, 29.72, 31.80, 31.95, 68.18, 69.01, 100.68, 112.27, 114.19, 114.83, 121.35, 121.68, 127.54, 130.75, 131.22, 144.64, 148.40, 157.64, 159.97, 161.46, 164.69, 186.31; ESI-MS 645.8 [M+H]⁺; Anal. Calc. for C₄₂H₆₀O₅; C, 78.22; H, 9.38; found: C, 78.29; H, 9.44%.

(E)-3-(3-(4-(octadecyloxy)phenyl)acryloyl)-7-(octyloxy)-2H-chromen-2-one (14e)



Yield : 86.87%; Melting Point : 122-124 °C; IR (KBr) : 2922, 2849, 1720, 1653, 1616, 1595, 1563, 1539, 1509, 1467, 1428, 1397, 1367, 1341, 1292, 1266, 1249, 1163, 1122, 1069, 1029, 1003, 987, 958, 870, 838, 805, 778, 753, 723, 641 cm^{-1} ; $^1\text{H-NMR}$ (400 MHz, CDCl_3) : δ ppm 0.88-0.93 (m, 6H), 1.27-1.31 (m, 36H), 1.43-1.49 (m, 4H), 1.81-1.86 (m, 4H), 4.00 (t, $J = 6.4\text{Hz}$, 2H), 4.06 (t, $J = 6.4\text{Hz}$, 2H), 6.85 (d, $J = 2.0\text{Hz}$, 1H), 6.90-6.94 (m, 3H), 7.56 (d, $J = 8.8\text{Hz}$, 1H), 7.64 (d, $J = 8.8\text{Hz}$, 2H), 7.85 (d, $J = 15.6\text{Hz}$, 1H), 7.93 (d, $J = 15.6\text{Hz}$, 1H), 8.60 (s, 1H) ; $^{13}\text{C-NMR}$ (100 MHz, CDCl_3) : δ ppm 14.13, 14.16, 22.67, 22.72, 25.94, 26.02, 28.90, 29.17, 29.22, 29.30, 29.40, 29.59, 29.62, 29.69, 29.73, 31.80, 31.95, 68.18, 69.01, 100.68, 112.27, 114.18, 114.83, 121.36, 121.69, 127.54, 130.75, 131.22, 144.63, 148.39, 157.64, 159.96, 161.46, 164.69, 186.31; ESI-MS: 673.9 $[\text{M}+\text{H}]^+$; Anal. Calc. for $\text{C}_{44}\text{H}_{64}\text{O}_5$; C, 78.53; H, 9.59; found: C, 78.61; H, 9.67%.

4.6 References

- [1] Gray, G. W. Handbook of Liquid Crystals, Fundamentals. Germany: Wiley, 1988.
- [2] Handbook of Liquid Crystals, 8 Volume Set..Germany: Wiley, 2014.
- [3] D. Andrienko, *J. Mol. Liq.*, **2018**, 267, 520,
- [4] G.H. Brown, J.W. Doane, V.D. Neff, Structure and Physical Properties of Liquid Crystals, **1970**.
- [5] J. Wyart, *Acta Crystallogr.*, **1963**, 16, 235.
- [6] H.T. Srinivasa, A.K.T. Mohammad, *Phase Transitions*, **2021**, 94, 256.
- [7] Y.S.K. Reddy, N. P. Lobob, T. Narasimhaswamy, *New J. Chem.*, **2018**, 42, 598-612.
- [8] N.K. Chudgar, S.N. Shah, *Liq. Cryst.*, **1989**, 4, 661.
- [9] B.T. Thaker, P.H. Patel, A.D. Vansadiya, J.B. Kanojjiya, *Mol. Cryst. Liq. Cryst.*, **2009**, 515, 135.
- [10] E.A. Bakr, M.H.A. Al-Jumaili, *Mol. Cryst. Liq. Cryst.*, **2020**, 710, 40.
- [11] H.T. Srinivasa, H.N. Harishkumar, B.S. Palakshamurthy, *J. Mol. Struct.*, **2017**, 1131, 97.
- [12] J.P. Van Meter, B.H. Klanderma, *Mol Cryst Liq Cryst.*, **1973**, 22, 271.
- [13] A.A. Merlo, A. Tavares, S. Khan, M.J. Leite Santos, S.R. Teixeira, *Liq. Cryst.*, **2018**, 45, 310.
- [14] A.T. Mohammad, M.H. Al-Mohammedi, M.Z. Ghdayeb, S.M. Husain Al-Majidi, *Liq. Cryst.*, **2020**, 47, 414.
- [15] A. Gowda, M. Kumar, S. Kumar, *Liq. Cryst.*, **2017**, 44, 1990.
- [16] P. Shah, R. Soni, S.S. Soman, *J. Mol. Liq.*, **2012**, 335, 116178.
- [17] A.E. Blatch, G.R. Luckhurst, *Liq. Cryst.*, **2000**, 27, 775.
- [18] M. G. Reddy, N. P. Lobo & T. Narasimhaswamy, *Liq. Cryst.*, **2016**, 43, 896.
- [19] J. W. Goodby, I.M. Saez, S.J. Cowling, J.S. Gasowska, R.A. MacDonald, S. Sia, P. Watson, K.J. Toyne, M. Hird, R.A. Lewis, S.-E. Lee, V. Vaschenko, *Liq. Cryst.*, **2009**, 36, 567.
- [20] J.W. Goodby, R.J. Mandle, E.J. Davis, T. Zhong, S.J. Cowling, *Liq. Cryst.*, **2015**, 42, 593.
- [21] S.Z. Mohammady, D.M. Aldhayan, M.A Alshammri, A.K Alshammari, Alazmi, M. Katariya, K.D.; Jaremko, M. Hagar, M. *Symmetry*, **2021**, 13, 1832.

- [22] J. Li, Y. Peng, G. Song, *Catal. Lett.* **2005**,102, 159.
- [23] M. Hagar, H.A. Ahmed, T.H. El-Sayed, R. Alnoman, *J. Mol. Liq.*, **2019**, 285, 96.
- [24] J. Godzwon, M.J. Sienkowska, Z. Galewski, *Acta Phys. Pol. A.*, **2008**, 113, 1145.
- [25] M. Amela-Cortés, B. Heinrîch, B. Donnio, K.E. Evans, C.W. Smith, D.W. Bruce, *J. Mater. Chem.*, **2011**, 21, 8427.
- [26] V. Jain, S. Kaur, G. Mohiuddin, S. Kaur, P. Kumar, *Liq. Cryst.*, **2022**, 49, 162.
- [27] H.A. Ahmed, M. M. Naoum, G.R. Saad, *Liq. Cryst.*, **2013**, 40, 914.
- [28] H.A. Ahmed, M. Hagar, G.R. Saad, *Liq. Cryst.*, **2019**, 46, 1611.
- [29] A.K.T. Mohammad, H.K. Mustafa, *Liq. Cryst.*, **2022**, 49, 354.
- [30] K. D. Katariya, K.J. Nakum, R. Soni, S. S. Soman, M. Hagar, *J. Mol. Liq.*, **2022**, 357, 119073.
- [31] K. D. Katariya, R. Soni, K.J. Nakum, S. S. Soman, M. Hagar, *J. Mol. Struct.* **2022**, 1262, 133043.
- [32] R. Soni, K. D. Katariya, K.J. Nakum, S. S. Soman, S. Nada, M. Hagar, *Liq. Cryst.*, **2023**, 50, 636.
- [33] H.A. Ahmed, M. Hagar, T.H. El-Sayed, R. B. Alnoman, *Liq. Cryst.*, **2019**, 46, 1.
- [34] S.D. Durgapal, R. Soni, S.S. Soman, A.K. Prajapati, *J. Mol. Liq.*, **2020**, 297, 111920.
- [35] K.D. Katariya, K.J. Nakum, M. Hagar, *Liq. Cryst.*, **2022**, 49, 312.
- [36] M. Hagar, H.A. Ahmed, G.R. Saad, *J. Mol. Liq.*, **2019**, 273, 266.